© 2022. Published by The Company of Biologists Ltd | Journal of Cell Science (2022) 135, jcs259546. doi:10.1242/jcs.259546

RESEARCH ARTICLE

Haspin participates in AURKB recruitment to centromeres and contributes to chromosome congression in male mouse meiosis

Inés Berenguer[1,*,¶], Pablo López-Jiménez[1,¶], Irene Mena[1,‡], Alberto Viera[1], Jesús Page[1], José González-Martínez[2], Carolina Maestre[2,§], Marcos Malumbres[2], José A. Suja[1,] and Rocío Gómez[1,**]**

ABSTRACT

Chromosome segregation requires that centromeres properly attach to spindle microtubules. This essential step regulates the accuracy of cell division and must therefore be precisely regulated. One of the main centromeric regulatory signaling pathways is the haspin-H3T3ph-chromosomal passenger complex (CPC) cascade, which is responsible for the recruitment of the CPC to the centromeres. During mitosis, the haspin kinase phosphorylates histone H3 at threonine 3 (H3T3ph), an essential epigenetic mark that recruits the CPC, in which the catalytic component is Aurora B kinase (AURKB). However, the centromeric haspin-H3T3ph-CPC pathway remains largely uncharacterized in mammalian male meiosis. We have analyzed haspin functions by either its chemical inhibition with LDN-192960 in cultured spermatocytes, or the ablation of the *Haspin* gene in *Haspin*$^{-/-}$ mice. Our studies suggest that haspin kinase activity is required for proper chromosome congression both during meiotic divisions and for the recruitment of Aurora B and kinesin MCAK (also known as KIF2C) to meiotic centromeres. However, the absence of H3T3ph histone mark does not alter borealin (or CDCA8) and SGO2 centromeric localization. These results add new and relevant information regarding the regulation of the haspin-H3T3ph-CPC pathway and centromere function during meiosis.

KEY WORDS: Meiosis, Centromere, Centrosome, Haspin, H3T3ph, Aurora B

INTRODUCTION

Chromosome mis-segregation during mitosis and meiosis lead to the appearance of aneuploidies, a hallmark cause of tumorigenesis, prenatal death or developmental abnormalities in vertebrates. Gain or loss of chromosomes often originates from dysregulation of centromere assembly, errors in kinetochore–microtubule interactions, or chromosome congression failures. These processes are highly regulated and well-orchestrated by several master regulators, such as PLK1 and Aurora kinase B (AURKB), which perform their role in both mitosis (Lukasiewicz and Lingle, 2009; Nikonova et al., 2013; Schmucker and Sumara, 2014) and meiosis (Alfaro et al., 2021; Wellard et al., 2021). A recently described regulator is the kinase haspin (encoded by germ cell-specific gene 2, *Gsg2*), which is an evolutionary conserved serine/threonine kinase (Cairo and Lacefield, 2020; Higgins, 2010) and was first described in mouse testis as a meiosis-specific gene, even though it is also expressed in somatic cells (Tanaka et al., 1999). Several substrates are known for this kinase, including histone H3 (through the phosphorylation at threonine 3, H3T3ph), histone macroH2A (through the phosphorylation at serine 137, macroH2AS137ph) and the kinetochore protein CENP-T (phosphorylated at threonine 57, CENP-T T57ph) (Dai and Higgins, 2005; Maiolica et al., 2014; Markaki et al., 2009).

Most studies about haspin have been conducted in somatic cells, in which it was described as the main regulator responsible for the recruitment of the chromosomal passenger complex (CPC) to the inner centromere domain (ICD) through the phosphorylation of H3T3 (Higgins, 2010; Wang et al., 2010). The CPC is a multiprotein complex that possesses Aurora kinase B (AURKB) as the enzymatic subunit, playing an essential role during the regulation of chromosome congression, segregation and cytokinesis (Krenn and Musacchio, 2015; van der Horst et al., 2015). The signaling network involving haspin-mediated H3T3ph and Bub1-mediated histone H2A phosphorylation at T120 (H2AT120ph) underlies the defined localization of AURKB at the mitotic ICD (Hadders et al., 2020; Liang et al., 2020). In somatic cells, haspin coupled to GFP was detected at the centrosomes and in the nucleus (Dai et al., 2006, 2005). During interphase, the haspin kinase is inactive (Ghenoiu et al., 2013), becoming later activated at prophase by two consecutive phosphorylations generated by CDK1 and PLK1 (Zhou et al., 2014). Once activated, haspin phosphorylates H3T3 from prophase to anaphase throughout the chromatin, being more concentrated at the centromeres in metaphase (Dai and Higgins, 2005). H3T3ph then recruits the CPC to the ICD through the baculovirus IAP repeat (BIR) domain of survivin (BIRC5) (Kelly et al., 2010). Once at the centromere, AURKB generates a positive feedback loop and phosphorylates haspin, promoting a higher accumulation of the CPC at centromeres (Wang et al., 2011). After AURKB is recruited to the centromeres, Shugoshin 2 (SGO2) and mitotic centromere-associated kinesin (MCAK, also known as KIF2C) are loaded (Huang et al., 2007). MCAK is a depolymerizing kinesin involved in the correction of improper kinetochore–MT attachments, which is recruited to the centromeres in an SGO2-dependent manner (Huang et al., 2007; Kline-Smith and Walczak, 2004). At the end of the mitotic metaphase, H3T3ph is dephosphorylated (Kelly et al., 2010) by the action of the PP1–Repo-Man complex and haspin is inactivated (Qian et al., 2013; Vagnarelli et al., 2011).

Since its discovery, several publications have reported functional studies about haspin in somatic cells. Haspin activity knockdown by

[1]Cell Biology Unit, Department of Biology, Universidad Autónoma de Madrid (UAM), 28049 Madrid, Spain. [2]Cell Division and Cancer group, Spanish National Cancer Research Centre (CNIO), 29029 Madrid, Spain.
*Present address: Department of Molecular Neuropathology, Molecular Biology Center Severo Ochoa (CBMSO), 28049 Madrid, Spain. ‡Present address: Institute for Behavioral Medicine Research, Wexner Medical Center, The Ohio State University, 43210 Columbus, OH, USA. §Present address: Molecular Oncology group, IMDEA Food Institute, CEI UAM+CSIC, 28049 Madrid, Spain.
¶These authors contributed equally to this work

**Authors for correspondence (jose.suja@uam.es; rocio.gomez@uam.es)

I.B., 0000-0002-7702-0611; P.L.-J., 0000-0002-6673-5996; I.M., 0000-0003-1200-1599; A.V., 0000-0002-3602-4130; J.P., 0000-0001-8381-324X; C.M., 0000-0003-2480-8082; M.M., 0000-0002-0829-6315; J.A.S., 0000-0002-4266-795X; R.G., 0000-0003-4408-9812

Handling Editor: David Glover
Received 2 November 2021; Accepted 6 June 2022

Journal of Cell Science (2022) 135, jcs259546. doi:10.1242/jcs.259546

RNAi induces the absence of H3T3ph and causes alterations in chromosome alignment (Dai et al., 2005) and premature loss of sister chromatid cohesion (SCC) (Dai et al., 2009, 2005), suggesting a role for this kinase in centromeric cohesion and pointing to a potential link with Shugoshin 1 (SGO1). In this sense, several works reported the colocalization of H3T3ph with the cohesin subunit SA2 (STAG2) (Dai et al., 2006) and also suggested the association of haspin with PDS5 proteins, regulators of SCC (Carretero et al., 2013; Liang et al., 2018; Yamagishi et al., 2010). On the other hand, the chemical inhibition of haspin kinase activity in somatic animal and plant cells using different inhibitors such as 5-iodotubercidin (5-Itu), CHR-6494 (CHR) and LDN-192960 (LDN) impairs AURKB localization to the centromeres (Cuny et al., 2012; Huertas et al., 2012; Patnaik et al., 2008; Wang et al., 2012). These data point to the involvement of haspin in the regulation of AURKB to fulfill chromosome segregation in mitosis (De Antoni et al., 2012; Kozgunova et al., 2016; Wang et al., 2012). Following this approach and the increasing development of chemical inhibitor drugs, strategies using haspin as an anti-cancer target are arising (Amoussou et al., 2018). Moreover, the upregulation of this kinase in some cancer cells has corroborated a central role for haspin in cell proliferation, increasing interest in haspin as a potential target for cancer treatment (Zhu et al., 2020).

Although most studies on haspin have focused on somatic cells, significantly fewer reports have been published about the distribution and functions of haspin in vertebrate meiosis (Cairo and Lacefield, 2020). During mouse oogenesis, haspin appears at centromeres and at sister chromatid axes at metaphase I and metaphase II, and at the midbody at anaphase I (Nguyen et al., 2014). Other immunolocalization assays detected this kinase through the entire chromatin of condensed bivalents during meiosis I (Wang et al., 2016). In mouse oogenesis, haspin is implicated in H3T3 phosphorylation, chromosome condensation, CPC localization at centromeres, microtubule-organizing center (MTOC) clustering and stability through Aurora kinase C (AURKC), and cytokinesis (Balboula et al., 2016; Nguyen et al., 2018; Quartuccio et al., 2017; Wang et al., 2016). Chemical inhibition of haspin by 5-Itu causes cell instability and clustering defects of acentriolar MTOCs in meiosis I (Balboula et al., 2016). These evolutionarily conserved functions of haspin kinases in mammals have also recently been reported in pig oocytes (Cao et al., 2019).

During male mouse meiosis, the sequence of loading of several centromeric and kinetochore proteins was reported, including the CPC components borealin (CDCA8), INCENP and AURKB, which load sequentially to the ICD before SGO2 and MCAK (Llano et al., 2008; Parra et al., 2009, 2006). However, although haspin expression was first identified in testis as a germ cell-specific gene (Tanaka et al., 1999), many questions about its functions in vertebrate male meiosis are still unsolved, and much fewer reports have been presented for spermatogenesis, for which recent data on the unique spatiotemporal pattern of histone H3 modifications implicate haspin in the epigenetic control of spermiogenesis (Soupsana et al., 2021).

As Aurora kinases (AURKs) are the main regulators of chromosome congression, segregation and cytokinesis, it is essential to unravel the signaling pathways that recruit them to the centromeres during vertebrate gametogenesis. In mammalian germ cells, two different AURKs (AURKB and AURKC) participate in the CPC (Balboula and Schindler, 2014; Shuda et al., 2009), and both can functionally regulate each other's localization and activity during oogenesis (Nguyen et al., 2018) or compensate for one another, ensuring successful mammalian spermatogenesis (Wellard et al., 2020). In this work, we examined the role of haspin in male mouse meiosis by using two strategies: chemical inhibition using LDN-192960 in wild-type (WT) cultured spermatocytes, and the analysis of a haspin knockout mouse model (*Haspin*$^{-/-}$). Both experimental approaches implicated haspin kinase activity in the regulation of chromosome congression, the recruitment of AURKB and the phosphorylation of AURKB at the ICD in both meiotic divisions. In addition, as haspin inhibition or ablation does not disturb SGO2 or borealin localization to the centromeres, our results suggest that the haspin-H3T3ph-AURKB/C pathway is not the only route to recruit CPC components to meiotic centromeres. In contrast, our results suggest that haspin is responsible for the recruitment of the kinesin MCAK to meiotic centromeres.

RESULTS

LDN-192960 is an efficient haspin inhibitor in mouse organotypic seminiferous tubule cultures

The distribution of the main target of haspin kinase, H3T3ph, was analyzed by immunolabeling in spermatocytes obtained from cultured seminiferous tubules, using the squashing protocol. This technique does not disturb either the tridimensionality of cell morphology, chromosome condensation or protein distribution in prophase I and dividing spermatocytes (Page et al., 1998; Parra et al., 2002). Labeling of the SYCP3 protein, the main component of the synaptonemal complex lateral elements, and DAPI staining were used as markers for the identification of meiosis substages, as previously reported (Parra et al., 2004). H3T3ph began to be detectable at diakinesis, presenting a heterogeneous faint distribution over the chromatin, with slightly more accumulation at chromocenters (clustered centromeres) (Fig. 1A,B). From prometaphase I (proM-I) to metaphase I (M-I), H3T3ph intensity progressively increased over the chromatin, being more intense at the interchromatid domains (Fig. 1C,D). In anaphase I (A-I), the H3T3ph signal became weaker (Fig. 1E) and it completely disappeared at the end of telophase I (T-I) (Fig. 1F). H3T3ph was not detected in interkinesis nuclei (Fig. 1G) but was again visible at the centromeric heterochromatin at prometaphase II (proM-II) (Fig. 1H), and completely marked the chromosomes from metaphase II (M-II) until the end of telophase II (T-II) (Fig. 1I–K). These data confirm that H3T3ph distribution in male mouse meiosis resembles the pattern described for mitosis, in which it was also located over the entire chromatin (Dai and Higgins, 2005).

We then analyzed the effect of haspin inhibition *in vitro*. LDN-192960 (LDN) has shown inhibitory effects on the proliferation of somatic cells owing to its action over the kinase activity of haspin (Amoussou et al., 2018; Huertas et al., 2012; Wang et al., 2012). To investigate whether this molecule shows activity in spermatocytes, we treated organotypic cultures of seminiferous tubules with increasing concentrations of LDN at different incubation times, using the haspin target H3T3ph as a marker (Dai and Higgins, 2005; Dai et al., 2005).

In somatic cell lines (HeLa and human osteosarcoma U2OS), the optimal efficient concentration of LDN used was 10 µM (Wang et al., 2012). However, we had to use higher concentrations due to the peculiarities of the organotypic culture, in which tubules are placed over an agarose gel (half-soaked) embedded in the medium. This means that the media does not surround the cells but, instead, the media diffuses to the seminiferous tubules via the agarose gel (Alfaro et al., 2021; Sato et al., 2011). We therefore decided to test higher concentrations of the inhibitor for 2, 4 and 6 h. Concentrations below 1 mM had no effect on meiosis progression or cell morphology, but conspicuous effects were observed with a 1 mM concentration (Fig. 2). These effects involved both alterations

Journal of Cell Science (2022) 135, jcs259546. doi:10.1242/jcs.259546

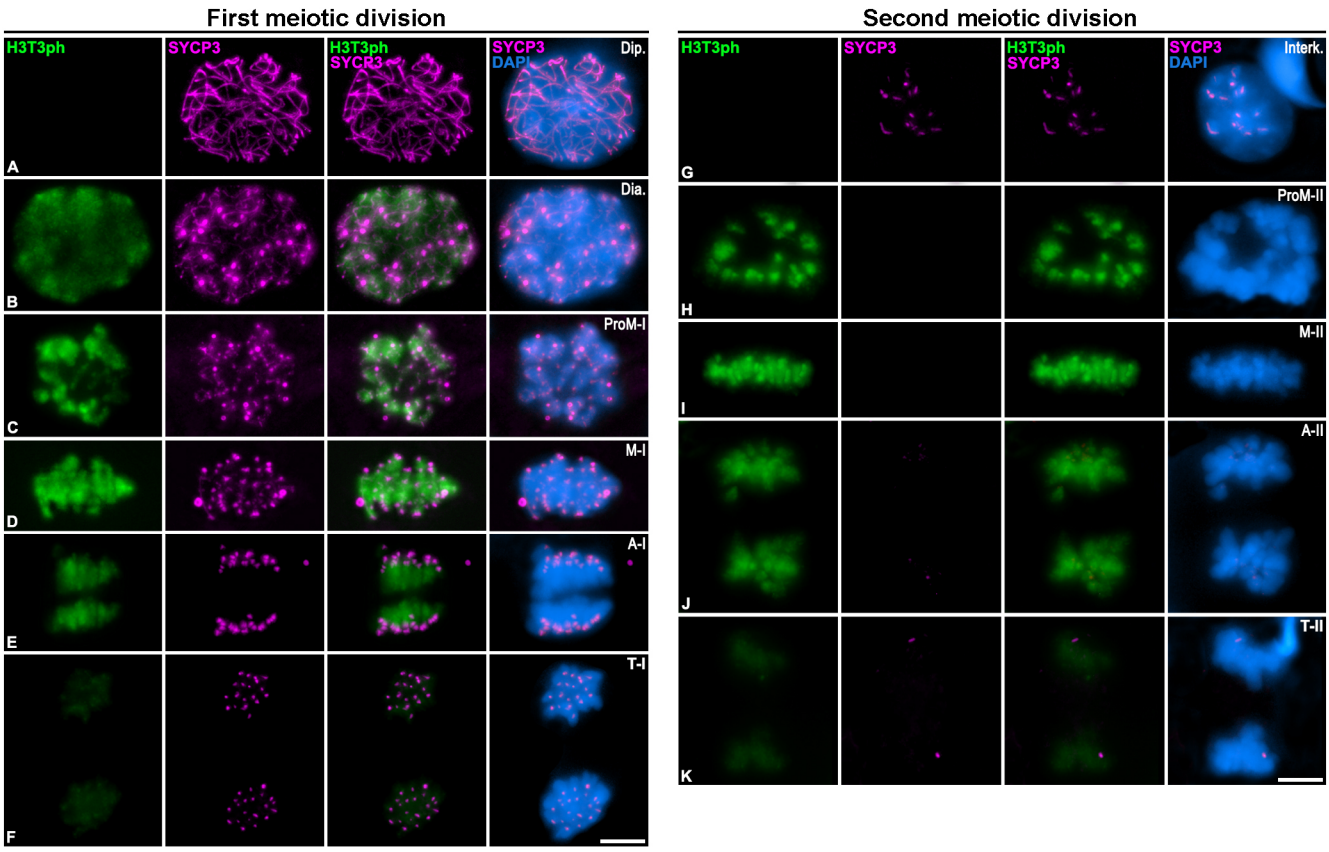

Fig. 1. Distribution of H3T3ph and SYCP3 during first and second meiotic division. Double immunolabeling of H3T3ph (green) and SYCP3 (magenta) on squashed WT mouse spermatocytes at (A) diplotene (Dip.), (B) diakinesis (Dia.), (C) prometaphase-I (ProM-I), (D) metaphase-I (M-I), (E) anaphase-I (A-I), (F) telophase-I (T-I), (G) interkinesis, (H) prometaphase-II (ProM-II), (I) metaphase-II (M-II), (J) anaphase-II (A-II) and (K) telophase-II (T-II). Chromatin was stained with DAPI (blue). Images are representative of 10 cells/stage in three different individuals. Scale bars: 10 µm.

in chromosome congression and the intensity of H3T3ph signals in M-I spermatocytes. Results revealed that 13.1% of M-I cells lacked H3T3ph signal after 2 h of treatment (Fig. 2Aa,Ab,B). In contrast, after 4 h of LDN treatment, we observed that H3T3ph signal was abolished in 97.9% of M-I cells (Fig. 2Ac,Ad,B,C). The total loss of H3T3 phosphorylation in M-I cells was achieved after 6 h LDN treatment (Fig. 2Ae,Af,B,C). These results confirmed that H3T3 phosphorylation by the haspin kinase was abolished in mouse spermatocytes with 1 mM LDN 6 h treatment. For this reason, all the subsequent analyses were performed using these culture conditions.

Haspin activity is required for proper chromosome congression in M-I and M-II spermatocytes

The effect of LDN was evident not only on the phosphorylation of H3T3, but also on the alignment of chromosomes at the metaphase plate. In order to better characterize this effect, we performed a quantitative analysis of the phenotypes seen in M-I and M-II spermatocytes after labeling H3T3ph and SYCP3 (for M-I) and H3T3ph and kinetochores (anti-centromere autoantibody, ACA) (for M-II). Spermatocytes were classified into three categories: aligned M-I or M-II (all bivalents or chromosomes are arranged at the equatorial plate), misaligned M-I or M-II (one or more bivalents or chromosomes are not in the equatorial plate) and apoptotic M-I or M-II [chromatin hypercondensation, no immunoreactivity and positive for the terminal deoxynucleotidyl transferase-mediated dUTP fluorescein nick-end labeling (TUNEL) assay apoptotic marker] (Fig. 2C; Fig. S1A). Apoptotic spermatocytes were identified by their size and morphology as M-I (Fig. S1Aa) or M-II (Fig. S1Ab). H3T3ph signals were clearly detected in control M-I (Fig. 2Ca) and M-II (Fig. 2Ce). In contrast, H3T3ph signals were absent in all LDN-treated M-I and M-II cells, regardless of whether they were classified as aligned or misaligned (Fig. 2C).

The quantitative analysis showed that LDN-treated cultures showed a three-fold increase in chromosome misalignment in M-I spermatocytes (74.7%) compared to control M-I cells (24.3%) and a two-fold increase in the rate of apoptosis (9%) (Fig. 2D). Similarly, the percentage of M-II cells with misaligned chromosomes rose two-fold in LDN-treated spermatocytes (62.3%), compared to control M-II cells (34.2%). For M-II cells, the apoptotic rate in LDN-treated spermatocytes (18.4%) was four-fold higher than in control ones (4.1%) (Fig. 2D). These data indicate that the disruption of haspin kinase activity causes a dramatic increase in alignment errors during M-I and M-II in mouse spermatocytes, potentially leading to cell death.

Haspin inhibition perturbs kinetochore–microtubule attachment in mouse M-I and M-II spermatocytes

As LDN treatment affects M-I and M-II bivalent or chromosome congression, we then studied the interaction between kinetochores and the meiotic spindle. Haspin involvement in MTOC organization has been previously reported in oocytes (Balboula et al., 2016). We therefore studied the dynamics of the meiotic spindle and the attachment of chromosomes to microtubules. For this purpose, we immunolabeled spermatocytes with α-tubulin and kinetochores (using ACA) (Fig. 3). M-I cells with correctly bi-oriented and aligned bivalents had bipolar spindles (Fig. 3Aa). In contrast, in

Journal of Cell Science (2022) 135, jcs259546. doi:10.1242/jcs.259546

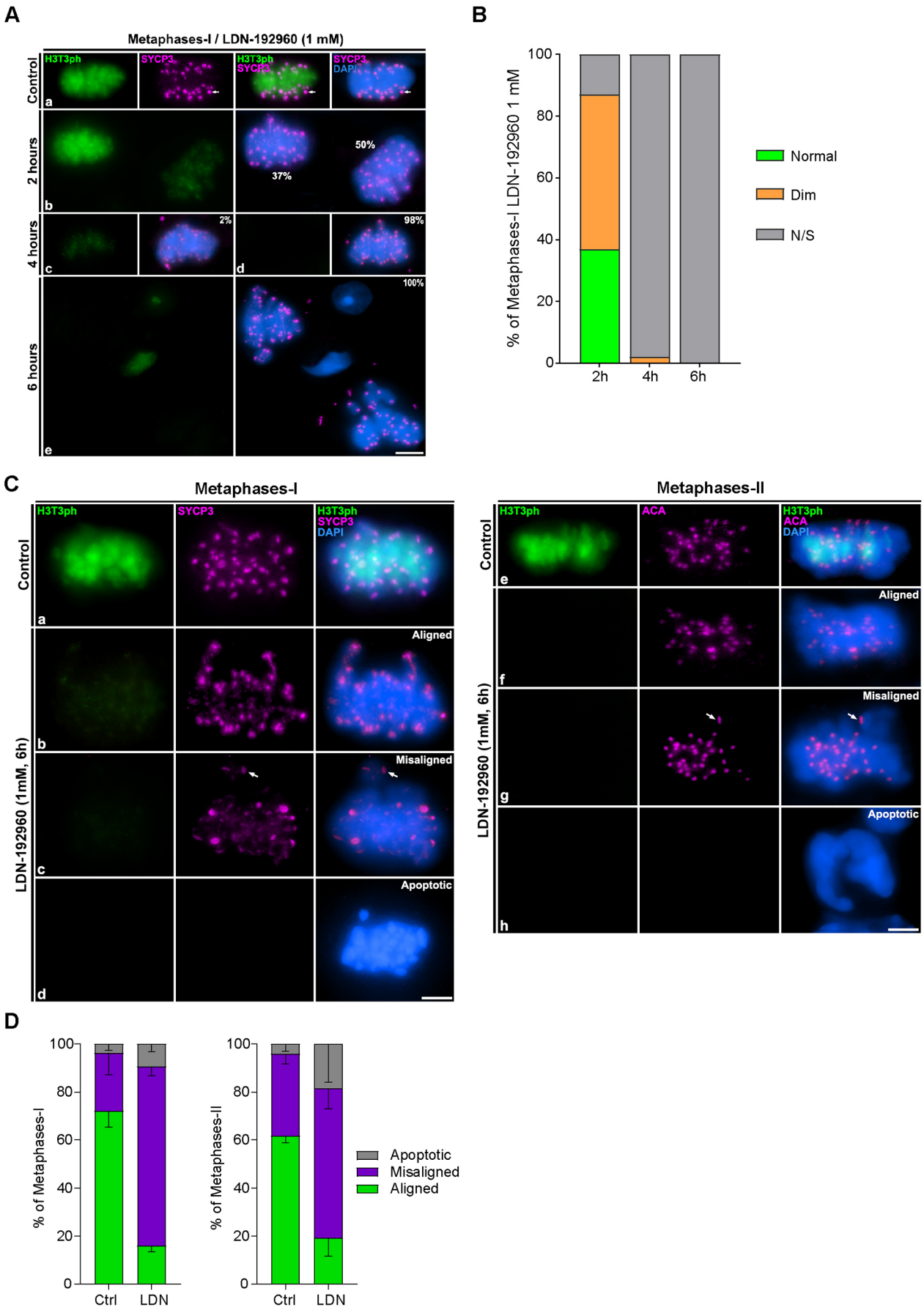

Fig. 2. See next page for legend.

Journal of Cell Science (2022) 135, jcs259546. doi:10.1242/jcs.259546

Fig. 2. Optimization of haspin inhibition in organotypic cultures of seminiferous tubules. (A) Double immunolabeling of H3T3ph (green) and SYCP3 (magenta) in squashed metaphase-I spermatocytes for (a) control and (b) 2 h, (c,d) 4 h and (e) 6 h treatment with 1 mM LDN-192960. Chromatin was stained with DAPI (blue). White arrows (a) indicate misaligned chromosomes, percentages of metaphases-I are shown (b–e). (B) Quantification of the percentages of metaphase I (M-I) cells with normal signals, dim signals or no signal (N/S) of H3T3ph in cultured seminiferous tubules with 2 h, 4 h and 6 h treatment with 1 mM of LDN-192960 (n=2). (C) H3T3ph distribution in control and 1 mM 6 h LDN-192960-treated metaphase-I and metaphase-II spermatocytes. Double immunolabeling of H3T3ph (green) and SYCP3 (magenta) in metaphase-I (a) control and (b–d) 6 h 1 mM LDN-192960-treated spermatocytes. Double immunolabeling of H3T3ph (green) and ACA (magenta) in (e) control and (f–h) 6 h 1 mM LDN-192960-treated metaphase-II spermatocytes. White arrows indicate a misaligned bivalent in Cc and a misaligned chromosome in Cg. Chromatin was stained with DAPI (blue). (D) Quantification of the incidence of misaligned metaphase-I and metaphase-II cells. Percentages of aligned, misaligned and apoptotic metaphase cells are represented for control and 1 mM LDN-192960 for 6 h treatment. Experiments were conducted in three different biological replicates. Bars and error bars represent mean±s.d. Scale bars: 10 µm.

misaligned M-I cells, some bivalents were not correctly anchored to the microtubules, usually remaining linked to only one pole (monotelic orientation) (Fig. 3Ab). A careful examination of these misaligned bivalents revealed that the two homologous kinetochores were usually attached to the same cellular pole (Fig. 3Bb′,Bb″). No apparent errors in SCC were detected, as univalents or independent chromatids were never observed.

A small proportion of LDN-treated M-I cells that had two or more misaligned bivalents usually presented tripolar spindles (Fig. 3Ac). The incidence of multipolar spindles in LDN-treated spermatocytes is low, 10.88% in M-I and 6.25% in M-II (Fig. 3C). These data suggest a possible impairment in centrosome dynamics or a potential off-target effect of the drug. Thus, we checked the localization of pericentrin (PCNT), a component of the pericentriolar matrix. In control M-I cells, PCNT appears as a compact mass on both poles of the cell (Alfaro et al., 2021). However, LDN-treated M-I cells presented alterations in PCNT distribution. In bipolar spindles, the signals appeared disaggregated, showing a variable number of pericentriolar matrix clusters with an irregular morphology (Fig. S2Aa,Ab). These features were also obvious in multipolar M-I or M-II cells (Fig. S2Ac,Ad). By looking at centrin 3 (CETN3), a marker of centrioles, multipolar cells were seen with abnormal centrioles at M-I (Fig. S2Bb) and M-II (Fig. S2Bc).

AURKB recruitment and AURKB/AURKC phosphorylation are reduced at centromeres when H3T3 phosphorylation is abolished

The phosphorylation of H3T3 is considered to be crucial for the recruitment of the CPC (Higgins, 2010; Wang et al., 2010). Therefore, downstream kinase AURKB recruitment is directly linked to haspin kinase activity (Krenn and Musacchio, 2015; van der Horst et al., 2015). AURKA, AURKB and AURKC belong to a family of kinases with high sequence homology (Tang et al., 2017). AURKA participates in centrosome dynamics in male mouse meiosis (Alfaro et al., 2021; Wellard et al., 2021), whereas AURKB and AURKC (hereafter denoted collectively as AURKB/C) function as the catalytic subunit of the CPC, presenting overlapping functions in spermatogenesis (Wellard et al., 2020).

As shown previously, H3T3ph decorated the chromatin in control M-I (Fig. 4Aa) and M-II (Fig. 4Ba), but this histone modification was absent when haspin kinase was inhibited with LDN in both M-I (Fig. 4Ab) and M-II (Fig. 4Bb). We then addressed whether AURKB was altered at the centromeres after haspin inhibition. The distribution of AURKB in mouse spermatocytes has been previously described (Parra et al., 2009, 2003). Our results showed that AURKB levels were reduced at the centromeres when haspin was inhibited with LDN in both M-I (Fig. 4Ac,Ad) and M-II (Fig. 4Bc,Bd). Quantification of the fluorescence signals showed a significant decrease in AURKB intensity at the centromeres both in M-I (Fig. 4C) and M-II (Fig. 4D). However, this also suggests that haspin kinase activity is not the only protein responsible for recruiting AURKB to centromeres.

We then used an antibody that detects the three Aurora kinases in their phosphorylated active form (AURKph). In control spermatocytes, this antibody mainly labeled centromeres and centrosomes during M-I and M-II, as well the midbody at T-I and T-II (Fig. S3). According to previous reports, these marks correspond to the localization of phosphorylated AURKB/C (AURKB/Cph) at centromeres (Nguyen and Schindler, 2017) and phosphorylated AURKA at the centrosomes (AURKAph) (Alfaro et al., 2021; Tang et al., 2017). To corroborate that this antibody indeed detects AURKA at the centrosomes, we performed co-immunolabeling with anti-CETN3 (Fig. S4). After haspin inhibition, the recruitment of AURKB/Cph to the ICD in M-I (Fig. 4Af) and in M-II (Fig. 4Bf) was also altered, as the intensity of labeling was fainter than in control spermatocytes (Fig. 4Ae,Be). Quantification of the fluorescence signals, associated with the chromosomes, showed a significant decrease in AURKB/Cph intensity at the centromeres both in M-I (Fig. 4C) and M-II (Fig. 4D).

Altogether, these data indicate the role of haspin kinase activity in AURKB recruitment and phosphorylation at the centromeres. The signals at the spindle poles in LDN-treated spermatocytes were similar to those found in control spermatocytes (white arrowheads in Fig. 4Ae,Af,Be,Bf), suggesting that AURKA phosphorylation might not be altered.

H3T3ph absence does not alter SGO2 loading to centromeres

Given the likely role of haspin in AURKB/C phosphorylation and recruitment to the centromeres, we then wondered whether SGO2, the protector of meiotic centromeric cohesion, might be affected. In mitosis, recruitment of Shugoshin proteins to centromeres requires the previous phosphorylation of H2A T120 by the kinetochore kinase Bub1 (Kawashima et al., 2010). With this in mind, we studied the distribution of SGO2 and its centromere docking mark H2AT120ph.

H2AT120ph appeared to be localized to the ICD of all chromosomes in both control (Fig. 4Ag) and LDN-treated M-I (Fig. 4Ah) cells. Similarly, SGO2 was present in the ICD of all chromosomes in control M-I (Fig. 4Ai) and also LDN-treated M-I (Fig. 4Aj). Signals of H2AT120ph and SGO2 in control and LDN-treated M-II were consistent in distribution and intensity (Fig. 4Bg–Bj). Quantification analysis showed no significant differences in H2AT120ph or SGO2 intensity at the centromeres between control and LDN inhibition in M-I (Fig. 4C) and M-II (Fig. 4D). These data suggest that the kinase activity of haspin does not have a direct role in the maintenance of the H2AT120ph-SGO2 pathway at centromeres in male mouse meiosis.

Haspin$^{-/-}$ mice are fertile but M-I and M-II spermatocytes lack centromeric H3T3ph and show alterations in chromosome alignment

To corroborate the *in vitro* results, we then analyzed the meiotic phenotype of a haspin knockout (KO) mouse model (*Haspin*$^{-/-}$) (Figs 5–8).

Journal of Cell Science (2022) 135, jcs259546. doi:10.1242/jcs.259546

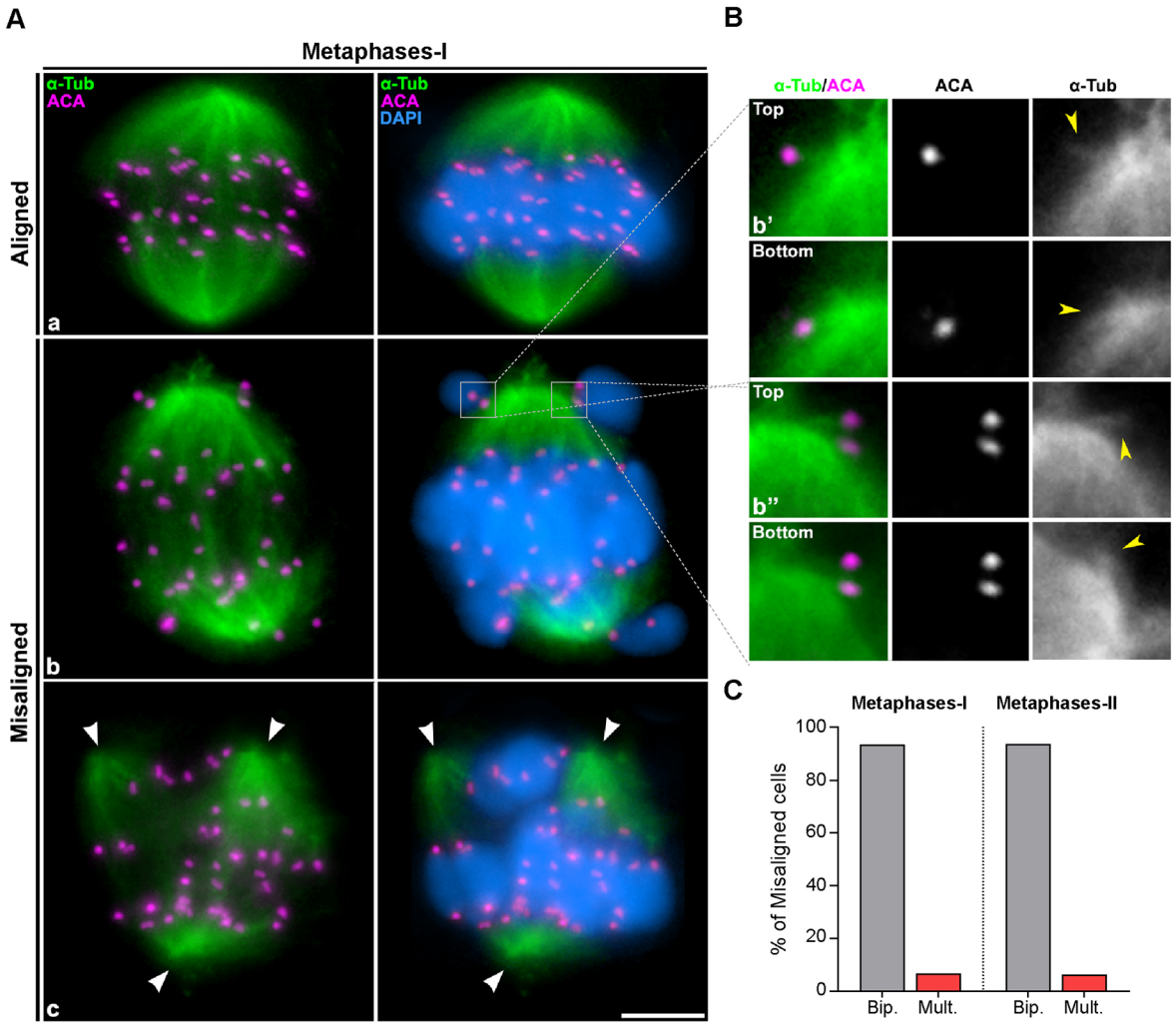

Fig. 3. Analysis of bivalent/chromosome congression in metaphase I and metaphase II after 1 mM 6 h LDN-192960 treatment. (A) Double immunolabeling of α-tubulin (green) and kinetochores (ACA) (magenta) in (a) aligned and (b,c) misaligned metaphase-I cells. White arrowheads in Ac indicate the spindle poles. Scale bar: 10 µm. (B) Kinetochore attachment of misaligned metaphase-I bivalents. Magnified views of the images in Ab are shown. Each image corresponds to the centromere of each homologous chromosomes (top and bottom). Yellow arrowheads indicate microtubule–kinetochore attachments. Chromatin was stained with DAPI (blue). Images are representative of 10 cells/stage in three different individuals. (C) Quantification of the percentage of bipolar (Bip.) and multipolar (Mult.) spindles in metaphase-I and -II spermatocytes with misaligned bivalents/chromosomes (*n*=3).

We analyzed the histology of the testes from *Haspin*$^{-/-}$ mice. Seminiferous tubules and the peritubular tissue in *Haspin*$^{-/-}$ mice seemed completely normal and spermatozoa could be observed in the epididymis (Fig. 5A); however, misaligned M-I cells were clearly observed (inset, Fig. 5A). This suggests an apparently normal fertility of these mutants, which was confirmed after crossing haspin-deficient males or females with WT mice. Both female and male *Haspin*$^{-/-}$ individuals were fertile, producing litter sizes not significantly different to those from *Haspin*$^{+/+}$ crossings (Fig. 5B). Additionally, we analyzed the sperm of *Haspin*$^{-/-}$ mice with the sperm chromatin dispersion (SCD) assay. We found no significant differences in DNA fragmentation in sperm from *Haspin*$^{+/+}$ and *Haspin*$^{-/-}$ males (Fig. 5C). *Haspin*$^{-/-}$ did not present univalents in M-I or independent chromatids in M-II, suggesting that SCC was not altered. To further analyze this, we detected the SMC3 cohesin subunit in *Haspin*$^{-/-}$ spread spermatocytes. No alterations were observed in SMC3 localization over the chromosomal axes, as seen by colabeling with axial/lateral elements of the synaptonemal complex stained with anti-SYCP3, in prophase-I spread spermatocytes (Fig. S5B) compared to *Haspin*$^{+/+}$ spread spermatocytes (Fig. S5A). SMC3 signals at the interchromatid domain in M-I in *Haspin*$^{-/-}$ were also identical to those in *Haspin*$^{+/+}$ (Fig. S5C,D). These data corroborate the fact that SCC is not directly regulated by haspin in male mouse meiosis.

In agreement with the *in vitro* experiments with LDN, we observed that H3T3ph is absent in the chromosomes of both M-I and M-II spermatocytes in *Haspin*$^{-/-}$ mice (Fig. 6A,B). Likewise, we reported an abundance of misaligned M-I and M-II cells. The frequency of these misaligned metaphases was also higher compared to WT, but slightly lower than that reported in our *in vitro* experiments (51.13% in M-I and 51.21% in M-II) (Fig. 6B). However, the frequency of apoptotic metaphases increased three-fold during M-I in *Haspin*$^{-/-}$ (25.42%) compared to *Haspin*$^{+/+}$ (8.5%), whereas LDN-treatment was only 2-fold higher in *Haspin*$^{-/-}$ than in control. The ratio of *Haspin*$^{-/-}$ apoptotic M-II (18%) was similar, but almost four-fold higher than in *Haspin*$^{+/+}$ (5.1%) (Fig. 6B). We confirmed that these metaphase cells were indeed apoptotic using the TUNEL assay (Fig. S1B). Surprisingly, multipolar metaphases were not observed

Journal of Cell Science (2022) 135, jcs259546. doi:10.1242/jcs.259546

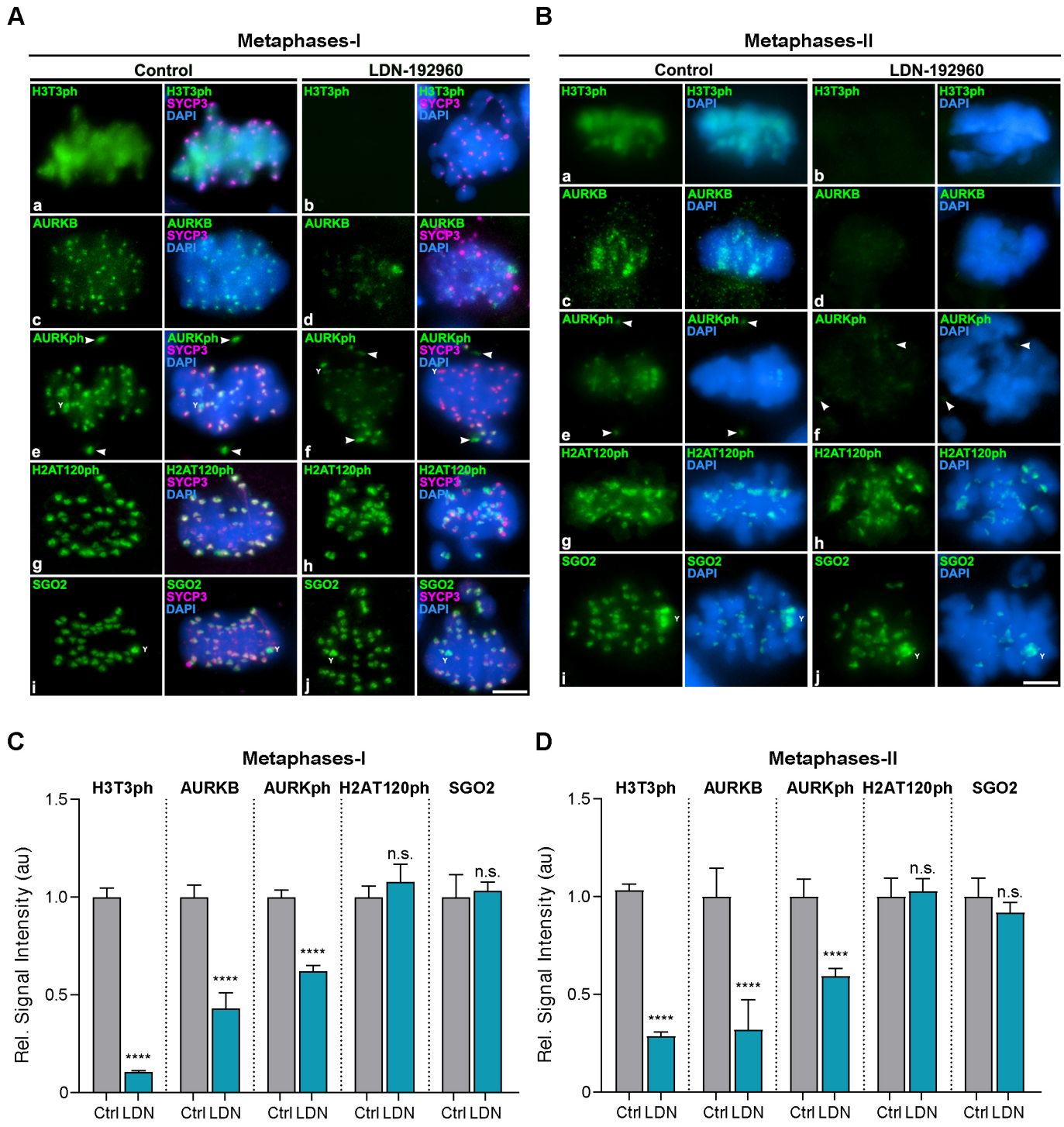

Fig. 4. Analysis of the inner centromere domain (ICD) in 6 h 1 mM LDN-192960-treated metaphase-I and metaphase-II spermatocytes. (A) Distribution of ICD components in metaphase-I spermatocytes. Double immunolabeling of SYCP3 (magenta) with either (a,b) H3T3ph (green), (c,d) AURKB (green), (e,f) AURKph (green), (g,h) H2AT120ph (green) or (i,j) SGO2 (green). (B) Distribution of ICD components in metaphase-II spermatocytes. Double immunolabeling of SYCP3 (magenta) with either (a,b) H3T3ph (green), (c,d) AURKB (green), (e,f) AURKph (green), (g,h) H2AT120ph (green) or (i,j) SGO2 (green). White arrowheads in Ae,Af,Be,Bf indicate the centrosomes. The centromere of chromosome Y is indicated (Y). Chromatin was stained with DAPI (blue). (C) Quantitative analysis of the relative signal intensities for different ICD components in metaphase-I spermatocytes. (D) Quantitative analysis of the relative signal intensity for different ICD components in metaphase-II spermatocytes. Experiments were conducted for one biological replicate. Data represent mean±s.e.m. au, arbitrary units. n.s., not significant; ****P<0.0001; two-tailed unpaired Student's t-test. Scale bars: 10 µm.

in cells from *Haspin*$^{-/-}$ mice. To ascertain whether multipolar spermatocytes from control mice under LDN treatment were caused by off-target effects, we then decided to treat *Haspin*$^{-/-}$ spermatocytes with the same LDN treatment (1 mM for 6 h). As we also observed multipolar M-I and M-II cells in *Haspin*$^{-/-}$ LDN-treated spermatocytes (Fig. S2C), the appearance of multipolar spermatocytes after LDN treatment seemed to be an off-target effect of the drug.

Journal of Cell Science (2022) 135, jcs259546. doi:10.1242/jcs.259546

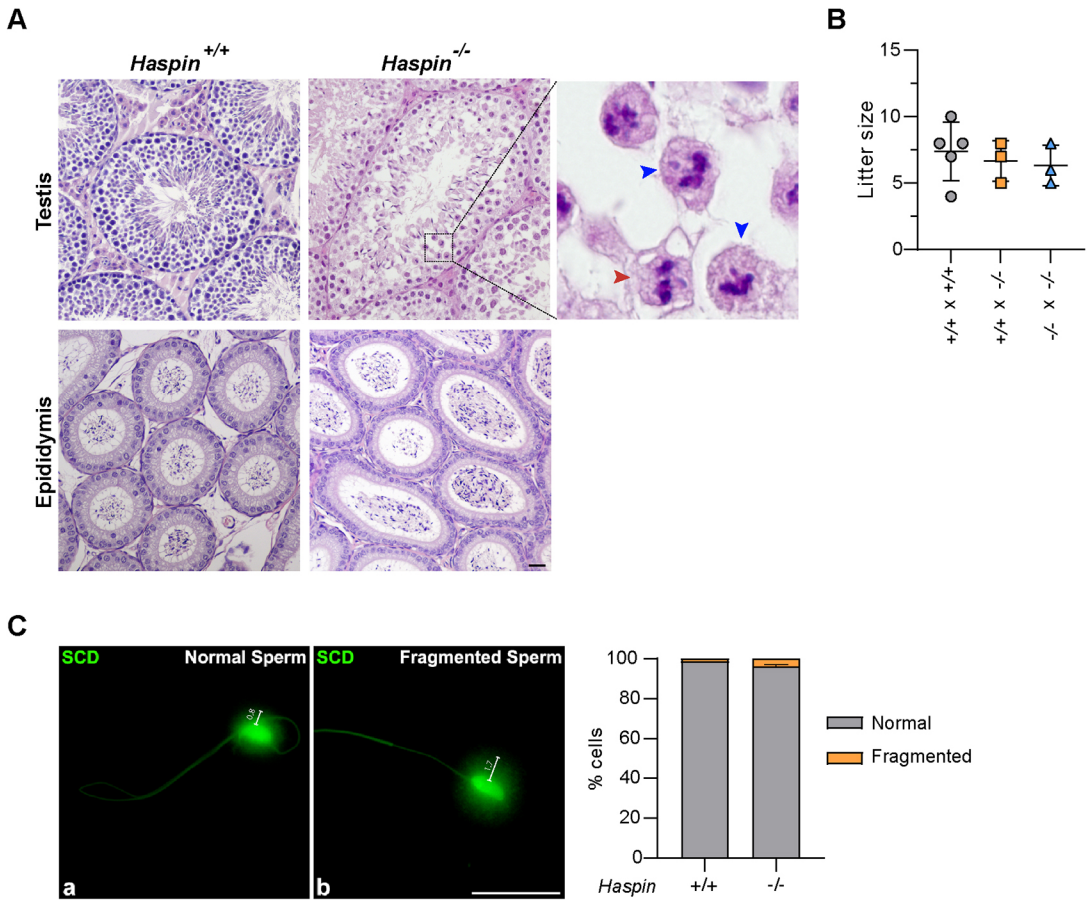

Fig. 5. Analysis of the fertility phenotype of the haspin knockout mouse model. (A) Hematoxylin and Eosin-stained histological sections of seminiferous tubules and epididymis from *Haspin*$^{+/+}$ *and Haspin*$^{-/-}$ mice. Scale bar: 200 µm. The magnified image shows a portion of a *Haspin*$^{-/-}$ seminiferous tubule with an aligned metaphase-I cell (red arrowhead) and two metaphase-I cells with misaligned bivalents (blue arrowheads). Images are representative of three sections/individual, and two individuals for each condition. (B) Litter sizes for crosses of male *Haspin*$^{+/+}$×female *Haspin*$^{+/+}$ mice, female *Haspin*$^{+/+}$×male *Haspin*$^{-/-}$ mice and male *Haspin*$^{-/-}$×female *Haspin*$^{-/-}$ mice. (C) Sperm chromatid dispersion (SCD) test in *Haspin*$^{+/+}$ and *Haspin*$^{-/-}$ spermatocytes. The values indicate the diameter of the chromatin fragmentation area. Scale bar: 10 µm. Graphical representation of spermatozoa with fragmented and non-fragmented DNA from *Haspin*$^{+/+}$ and *Haspin*$^{-/-}$ mice (*n*=1 and *n*=3 mice, respectively).

We analyzed the localization of the ICD components in *Haspin*$^{-/-}$ metaphase spermatocytes. We observed the absence of H3T3ph in *Haspin*$^{-/-}$ M-I (Fig. 7Aa,Ab,C) and M-II (Fig. 7Ba,Bb,D) cells. The absence of H3T3ph was accompanied by a significant reduction of AURKB and AURKB/Cph at centromeres in M-I (Fig. 7Ac–Af,C) and M-II (Fig. 7Bc–Bf,D) cells. In contrast, both H2AT120ph and SGO2 abundance were unaltered in M-I (Fig. 7Ag–Aj,C) and M-II (Fig. 7Bg–Bj,D) cells, as in LDN-treated spermatocytes. Quantification analysis showed no significant differences in H2AT120ph or SGO2 intensity at the centromeres between *Haspin*$^{+/+}$ and *Haspin*$^{-/-}$ in M-I (Fig. 7C) and M-II (Fig. 7D).

To further analyze other related proteins, we decided to study the CPC component borealin and the kinesin MCAK. Borealin has been described to be loaded to the centromere before AURKB, whereas MCAK is loaded after (Parra et al., 2009, 2003). We observed no significant alteration of borealin centromeric signals in *Haspin*$^{-/-}$ M-I spermatocytes (Fig. 8A), suggesting that the loading of this protein is not affected by the absence of the haspin kinase. In contrast, we observed a clear delocalization of the kinesin MCAK, which failed to be recruited to *Haspin*$^{-/-}$ M-I centromeres, presenting a relocalization presumably to the meiotic spindle (Fig. 8B). These data suggest that the haspin kinase is implicated in the loading of MCAK to centromeres during male mouse meiosis.

Finally, we analyzed another AURKB target, phosphorylation of histone H3 at S10 (H3S10ph), to check whether it was altered in *Haspin*$^{-/-}$ spermatocytes. No significant differences were observed for the intensity of H3S10ph between *Haspin*$^{+/+}$ and *Haspin*$^{-/-}$ M-I spermatocytes (Fig. 8C).

DISCUSSION

The role of haspin has been widely investigated in somatic cells. This kinase was found to be responsible for H3T3 phosphorylation, which is a necessary step for the proper loading of the CPC to the centromeres, chromosome alignment and SCC (Dai and Higgins, 2005; Maiolica et al., 2014; Markaki et al., 2009). Here, we report that some of these functions are also conserved in male meiosis, although important differences were found, indicating a possible redundancy of pathways in the correct assembly of the ICD in vertebrate meiosis. The two approaches used here, the functional *in vitro* inhibition of haspin with LDN and the use of a knockout mouse modelm produced congruent results, indicating the accuracy of these methods to assess haspin function in male meiosis.

Journal of Cell Science (2022) 135, jcs259546. doi:10.1242/jcs.259546

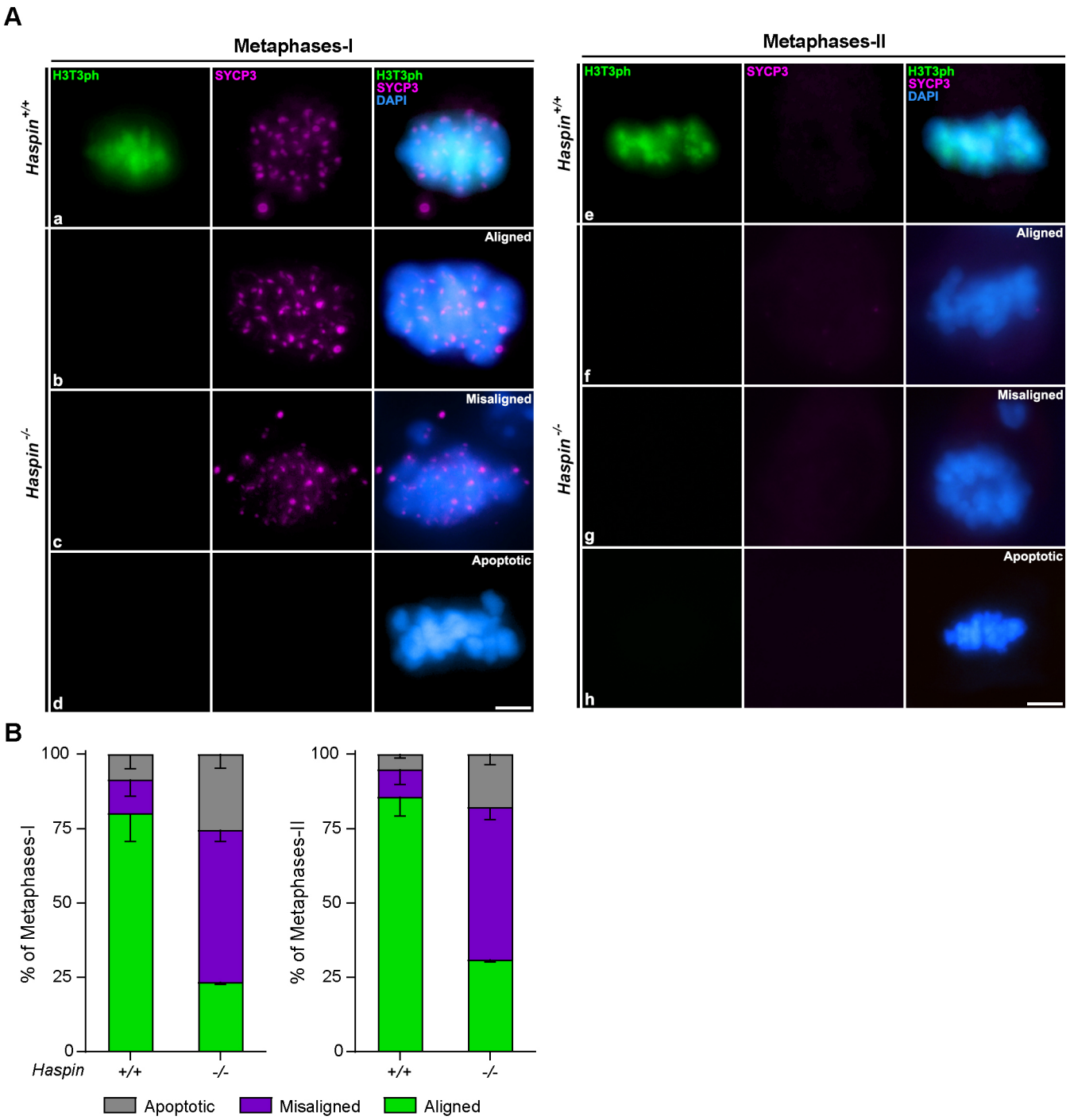

Fig. 6. Analysis of the meiotic phenotype of the haspin knockout mouse model. (A) Distribution of H3T3ph in *Haspin*$^{+/+}$ *and Haspin*$^{-/-}$ metaphase-I and metaphase-II spermatocytes. Double immunolabeling of H3T3ph (green) and SYCP3 (magenta). Chromatin was stained with DAPI (blue). Scale bars: 10 µm. (B) Quantification of the incidence of misaligned metaphase-I and metaphase-II. Percentages of aligned, misaligned and apoptotic metaphases are represented for *Haspin*$^{+/+}$ and *Haspin*$^{-/-}$ spermatocytes. Experiments were conducted in two different biological replicates. Bars and error bars represent mean±s.d.

Haspin facilitates proper chromosome congression in male mouse meiotic divisions by phosphorylating H3T3 and recruiting AURKB at centromeres, but is dispensable for the loading of borealin and SGO2 to the ICD

In the past years, several reports suggested that the CPC, including AURKB, must locate to the ICD to ensure accurate chromosome congression at the metaphase plate (Hindriksen et al., 2017; Kelly et al., 2010; Santaguida et al., 2010; Saurin et al., 2011; Wang et al., 2010). The current model proposes that the CPC is recruited to the chromatin regions where H3T3ph and H2AT120ph are present (Yamagishi et al., 2010), implying that the ICD might be defined by simultaneous interactions of the CPC with H3T3ph, H2AT120ph and SGO1/SGO2 (Hadders et al., 2020; Krenn and Musacchio, 2015; Liang et al., 2020). Interestingly, a recent model suggested that the ICD is scaffolded by a spatially regulated CPC, which is able to assemble and disassemble, allowing histone modifications to interact with each other during the different stages of the cell cycle (Trivedi and Stukenberg, 2020). In this regard, several publications

Journal of Cell Science (2022) 135, jcs259546. doi:10.1242/jcs.259546

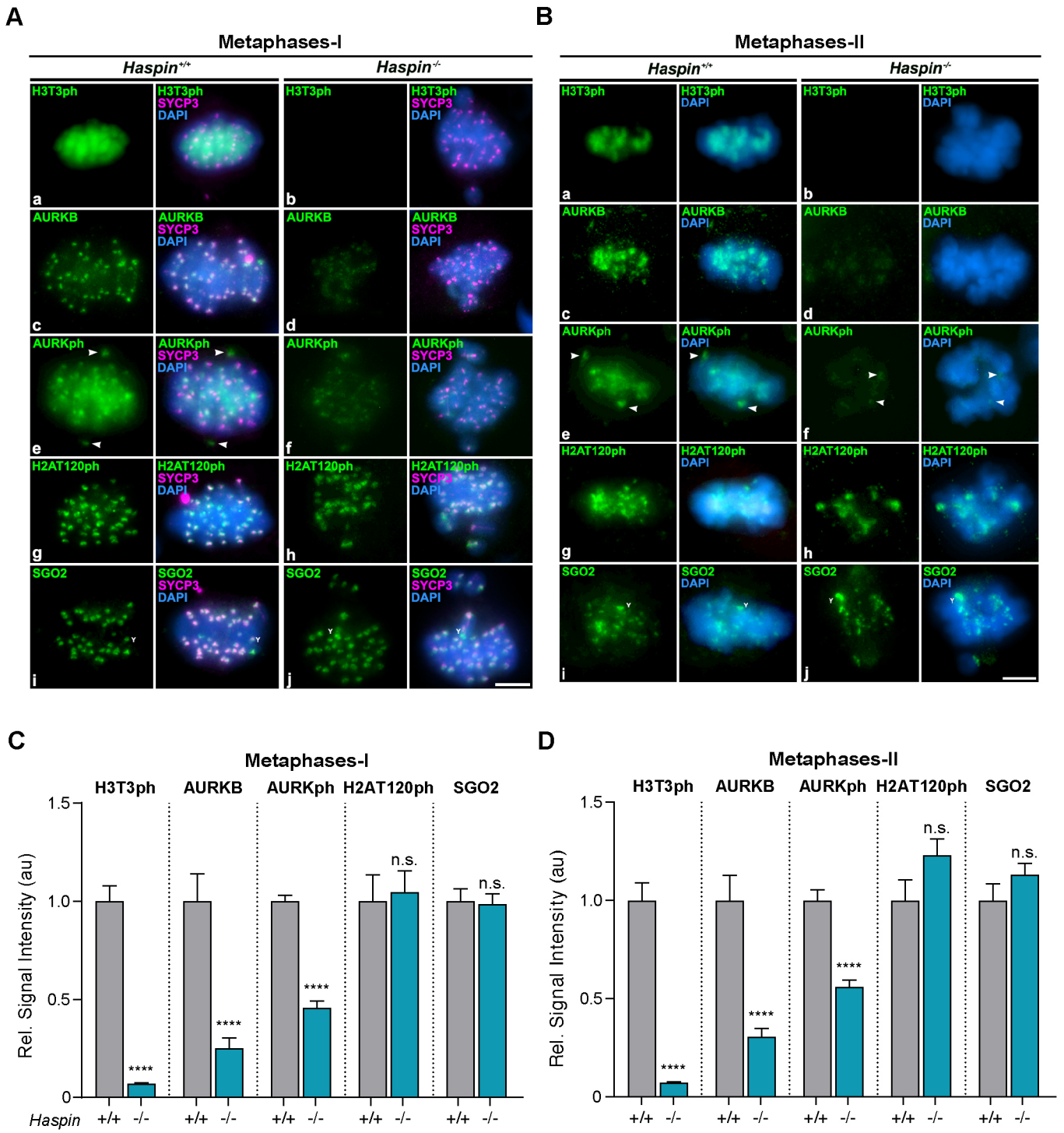

Fig. 7. Analysis of the inner centromere domain (ICD) in *Haspin*$^{+/+}$ and *Haspin*$^{-/-}$ metaphase-I and metaphase-II spermatocytes. (A) Distribution of ICD components in metaphase-I spermatocytes. Double immunolabeling of SYCP3 (magenta) with either (a,b) H3T3ph (green), (c,d) AURKB (green), (e,f) AURKph (green), (g,h) H2AT120ph (green) or (i,j) SGO2 (green). (B) Distribution of ICD components at metaphase-II spermatocytes. Double immunolabeling of SYCP3 (magenta) and either (a,b) H3T3ph (green), (c,d) AURKB (green), (e,f) AURKph (green), (g,h) H2AT120ph (green) or (i,j) SGO2 (green). White arrowheads in Ae, Be,Bf indicate the centrosomes. Chromatin was stained with DAPI (blue). The centromere of chromosome Y is indicated (Y). (C) Quantitative analysis of the relative signal intensity for different ICD components in metaphase-I spermatocytes. (D) Quantitative analysis of the relative signal intensity for different ICD components in metaphase-II spermatocytes. Experiments were conducted for two biological replicates. Data represent mean±s.e.m. au, arbitrary units. n.s., not significant; ****P<0.0001, two-tailed unpaired Student's t-test. Scale bars: 10 µm.

support the idea of different routes to recruit AURKB to mitotic centromeres. Broad and coworkers investigated three discrete AURKB populations at mitotic centromeres: an ICD pool of AURKB would be recruited by haspin-mediated phosphorylation of histone H3T3; a second pool, located at the kinetochores, would be recruited by Bub1-mediated phosphorylation of histone H2AT120; and a third pool would be recruited to the outer kinetochore by the protein CENP-C in early mitosis, independently of either the

Journal of Cell Science (2022) 135, jcs259546. doi:10.1242/jcs.259546

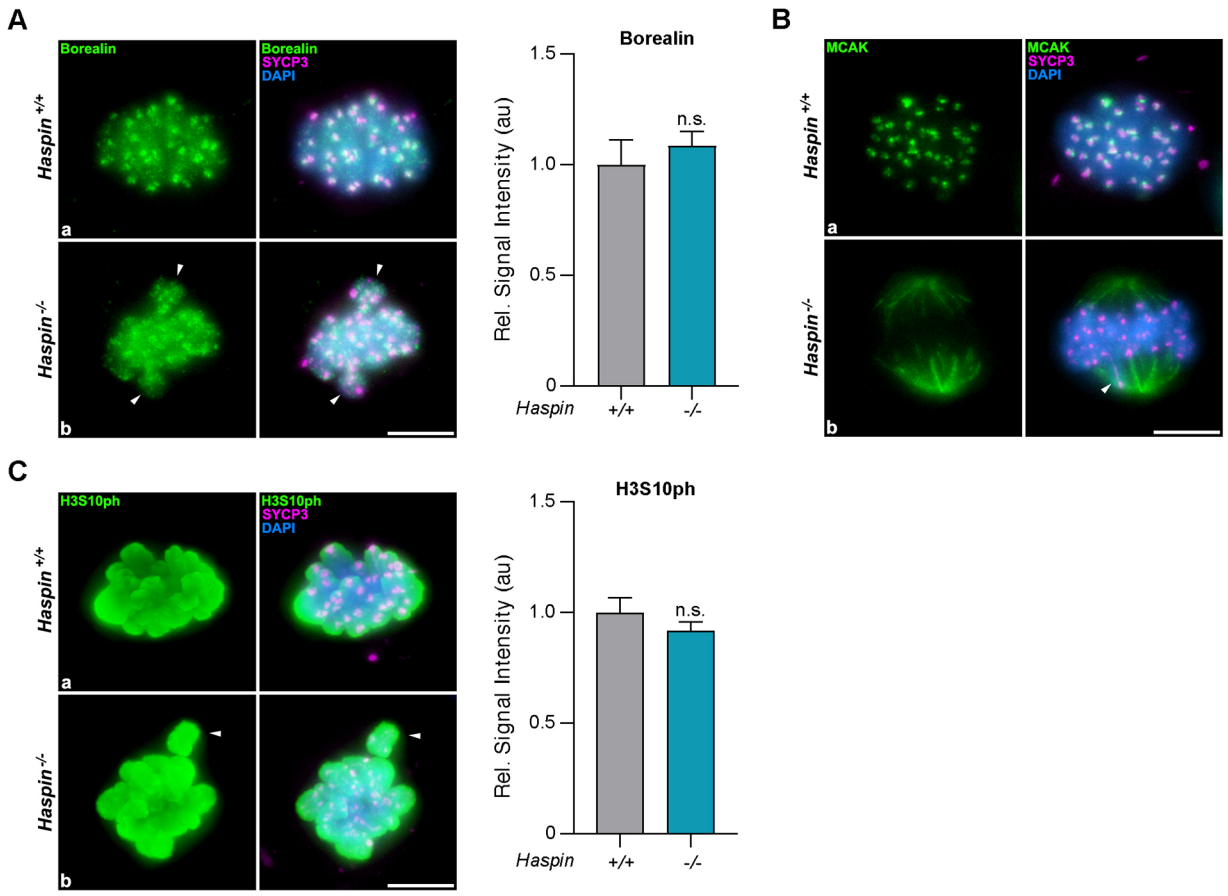

Fig. 8. Analysis of the chromosomal passenger complex (CPC) proteins borealin, kinesin MCAK and histone mark H3S10ph in *Haspin*$^{+/+}$ and *Haspin*$^{-/-}$ metaphase-I spermatocytes. (A) Double immunolabeling of borealin (green) and SYCP3 (magenta) in *Haspin*$^{+/+}$ (a) and *Haspin*$^{-/-}$ (b) metaphase-I spermatocytes. Chromatin was stained with DAPI (blue). White arrowheads in Ab point to misaligned bivalents. Graph represents the relative signal intensity of borealin signal in *Haspin*$^{+/+}$ and *Haspin*$^{-/-}$ metaphase-I spermatocytes. Analysis was conducted for one biological replicate. (B) Double immunolabeling of MCAK (green) and SYCP3 (magenta) in *Haspin*$^{+/+}$ (a) and *Haspin*$^{-/-}$ (b) spermatocytes. Analysis of MCAK distribution was conducted in three *Haspin*$^{-/-}$ biological replicates. Chromatin was stained with DAPI (blue). (C) Double immunolabeling of H3S10ph (green) and SYCP3 (magenta) in *Haspin*$^{+/+}$ (a) and *Haspin*$^{-/-}$ (b) spermatocytes. White arrowheads in Cb point to misaligned bivalents. Chromatin was stained with DAPI (blue). Graph represents the quantitative analysis of H3S10ph signals in metaphase-I spermatocytes. Analysis was conducted for one biological replicate. Data represent mean±s.e.m. au, arbitrary units. n.s., not significant; two-tailed unpaired Student's *t*-test. Scale bars: 10 µm.

Bub1-H2AT120ph-SGO1 or haspin-H3T3ph pathways (Broad et al., 2020). Furthermore, two additional publications demonstrated that the kinase activity of either haspin or Bub1 is sufficient to recruit AURKB to mitotic centromeres (Hadders et al., 2020; Liang et al., 2020), suggesting that the Bub1-H2AT120ph and haspin-H3T3ph pathways coexist in the ICD and have combined actions that ensure the recruitment of different pools of AURKB to the centromeres.

The results presented here are congruent with the involvement of haspin in the proper assembly of the ICD during meiosis and, interestingly, also suggest a redundancy of pathways in some steps of this process. Centromere dynamics are clearly altered in the absence (*Haspin*$^{-/-}$ spermatocytes) or inhibition (LDN-treated spermatocytes) of haspin kinase activity. The most conspicuous effects are the abolition of H3T3ph signals and the reduction of AURKB and AURKph signals at the centromeres in both meiotic divisions.

Our results suggest that H3T3ph and AURKph disruption at the centromeres leads to a malfunction of male meiotic progression, as revealed by the increase of misaligned chromosomes and apoptotic cells in both M-I and M-II. Therefore, haspin might play a fundamental role in ensuring proper chromosome congression or segregation in mouse gametogenesis: in both spermatogenesis and oogenesis. However, it appears that the role of haspin might be redundant with other proteins as neither haspin absence (*Haspin*$^{-/-}$) nor inhibition (LDN treatment) alter SGO2 localization to meiotic centromeres. These findings could imply a similar pathway for centromeric CPC regulation in meiosis in both sexes, as the retention of AURKB/C and SGO2 at centromeres after the inactivation of haspin is identical to what is seen in oocytes (Nguyen et al., 2014). This points to a similar pathway for CPC regulation in both spermatogenesis and oogenesis, and an alternative pathway capable of recruiting SGO2 to the ICD, at least during male mouse meiosis (Gómez et al., 2007; Llano et al., 2008). In mitosis, AURKB phosphorylates SGO2 (Tanno et al., 2010). Moreover, the inhibition of Bub1 kinase activity in haspin-deficient cells abolished any detectable enrichment of AURKB at centromeres (Liang et al., 2020). The few data available about mammalian gametogenesis indicate that, in mouse oocytes, the kinase activity of Bub1 is dispensable for SGO2 localization at the centromeres (El Yakoubi et al., 2017). Here, we show that although the haspin kinase is responsible for the recruitment of phosphorylated AURKB/C at centromeres, abolition of the haspin-H3T3ph pathway does not preclude the recruitment of SGO2 to the ICD. Consequently, we propose that in mouse

Journal of Cell Science (2022) 135, jcs259546. doi:10.1242/jcs.259546

spermatogenesis, the Bub1-H2AT120ph-SGO2 and haspin-H3T3ph-CPC pathways might also have redundant functions in the assembly of the CPC at centromeres. The fact that *Haspin*$^{-/-}$ mice are fertile despite the absence of H3T3ph and the reduction of AURKB phosphorylation at centromeres supports this hypothesis. Moreover, given that either the haspin or Bub1 kinase could independently recruit different pools of AURKB to support faithful chromosome segregation in mitosis (Hadders et al., 2020; Liang et al., 2020), we could hypothesize that, in spermatogenesis, there might also be different pools of AURKB at the inner centromere that synergistically ensure chromosome congression in meiosis. Intriguingly, a third AURK (AURKC) is involved in meiosis compared to mitosis (Brown et al., 2004; Nguyen and Schindler, 2017). Therefore, given that haspin inhibition does not perturb the spindle assembly checkpoint activity during female mammalian meiosis I in *Aurkc*$^{-/-}$ mice (Quartuccio et al., 2017) and that AURKB and AURKC have collaborative functions in oogenesis (Nguyen et al., 2018) and spermatogenesis (Wellard et al., 2020), we argue that the haspin–AURKB interaction might be dispensable and compensated by AURKC function during spermatogenesis. Ultimately, all these data point to a haspin-dependent, centromeric AURKB function in the context of chromosome congression regulation, which might have synergic functions with centromeric AURKC in male mouse meiosis.

However, other mitotic CPC components have been found to be altered by haspin activity. H3T3ph phosphorylation by haspin creates a chromatin-binding site for the BIR domain of survivin (Kelly et al., 2010; Wang et al., 2010; Yamagishi et al., 2010; Wang et al., 2012) and haspin RNAi causes CPC loss from centromeres but not the central spindle (Wang et al., 2010). Our results show that although AURKB and AURKB/Cph are reduced in LDN-treated *Haspin*$^{-/-}$ spermatocytes, the loading of borealin to centromeres is not affected. This is consistent with previous results describing the sequential assembly of centromeric proteins in male mouse meiosis, in which borealin is loaded to the centromeres before AURKB (Parra et al., 2009). Moreover, our data demonstrate that borealin loading to the centromeres is independent of haspin activity and, therefore, of H3T3ph. This idea is strengthened with data from oocytes, in which the presence of INCENP and survivin at centromeres is not affected by haspin inactivation (Nguyen et al., 2014). All these data reinforce the idea that mouse meiosis compiles a complex entangle of centromeric routes assembling the ICD.

Altogether, our work suggests that during spermatogenesis, the haspin-H3T3ph pathway is not the only route to recruit CPC components to the meiotic centromeres and is dispensable for the loading of borealin and SGO2 to centromeres in male mouse meiosis. Instead of converging to accumulate the CPC precisely at the ICD, haspin and Bub1 might each also recruit a separate functional CPC pool to the centromere, potentially sharing similarities with the mitotic centromeric pathway (Broad et al., 2020).

Haspin and AURKB are involved in the loading of MCAK to meiotic centromeres

Our results suggest that the presence of haspin is a prerequisite for the loading of MCAK to centromeres. Delocalization of MCAK from centromeres and relocalization to the meiotic spindle could further explain the appearance of misaligned bivalents or chromosomes in the absence of haspin, as this depolymerizing kinesin is responsible for correcting incorrect kinetochore–microtubule attachments (Ritter et al., 2015). In mitosis, haspin appears to influence MCAK localization and checkpoint signaling at centromeres by controlling AURKB localization (Qiao et al., 2014; Wang et al., 2010, 2012). Moreover, synergistic inhibition of AURKA and haspin disrupts the mitotic centromere aggregation of AURKB and MCAK (Chen et al., 2021). Taking into account that MCAK is loaded to centromeres in a SGO2-dependent manner in male meiosis (Llano et al., 2008), our results suggest that the presence of haspin at the ICD is a prerequisite for the recruitment of MCAK to the ICD. This suggests that phosphorylation of H3T3 precedes the appearance of AURKB and AURKB/Cph at centromeres, which in turn occurs prior to SGO2 and MCAK loading, in accordance with previous reports (Parra et al., 2009). Given that SGO2 localization is not altered in the absence or inactivation of haspin in spermatocytes, we suggest that MCAK recruitment depends on the presence and phosphorylation of AURKB at centromeres in male mouse meiosis. Therefore, we argue that in the absence of AURKB activity at the centromere, MCAK relocalizes to the meiotic spindle. Accordingly, several previous reports demonstrated that AURKB controls centromere localization of MCAK in somatic cells (Gorbsky, 2004; Lan et al., 2004; McHugh et al., 2019; Ohi et al., 2004), in which disruption of Aurora B function by expression of a kinase-dead mutant or RNAi also prevented centromeric targeting of MCAK, which relocalized to the mitotic spindle (Andrews et al., 2004).

Haspin is not implicated in the phosphorylation of H3S10 nor in SCC in male mouse meiosis

AURKB phosphorylates multiple substrates, including histone H3 at serine 10 (H3S10ph) on chromatin (Ruchaud et al., 2007). Our results showed that haspin kinase activity is not directly implicated in the phosphorylation of H3S10 in dividing spermatocytes, as this mark is not altered in metaphases either in the *in vitro* LDN experiments or in the *Haspin*$^{-/-}$ mouse model. Accordingly, AURKB-dependent H3S10 phosphorylation precedes H3T3 phosphorylation in G2 (Hirota et al., 2005; Ruppert et al., 2018) and H3S10ph is insensitive to the haspin inhibitor (Wang et al., 2012) in somatic cells.

However, it has been suggested that haspin depletion has similar effects compared to depletions of cohesion factors, as somatic *haspin*-depleted cells show premature loss of cohesion, leading to sister chromatid separation and prolonged mitotic arrest (Dai et al., 2009, 2006). In contrast, our results showed that SCC, at least mediated by SMC3-containing cohesin complexes, is not altered by either haspin inhibition or ablation. In addition, neither LDN-treated nor *Haspin*$^{-/-}$ spermatocytes present univalents in M-I or single chromatids in M-II. This indicates that haspin is not a major regulator of SCC in male mouse meiosis. These findings are further supported by observations in female mouse meiosis, in which SCC is also still intact after haspin inhibition in oocytes (Nguyen et al., 2014; Quartuccio et al., 2017).

Haspin is not directly implicated in centrosome dynamics in male mouse meiosis

Several studies have suggested that haspin inhibition causes MTOC instability in somatic cells and oocytes. In mitosis (U2OS cells), eGFP–haspin was detected at centrosomes (Dai et al., 2005) and further analysis showed that haspin knockdown with siRNA increased the number of centrosome-like foci that contained γ-tubulin and allowed microtubule polymerization (Dai et al., 2009). However, an increased incidence of MTOC foci in M-I spindles was also observed when analyzing haspin functions in mouse oocytes using inhibitors and overexpression approaches (Nguyen et al., 2014). Other results indicated that after haspin *in vitro* inhibition, the multiple MTOC foci that should cluster into two

Journal of Cell Science (2022) 135, jcs259546. doi:10.1242/jcs.259546

poles failed to do so, albeit the MTOC localization of AURKA was not perturbed (Balboula et al., 2016).

Our results demonstrate that LDN is an effective haspin inhibitor as it disturbs H3T3 phosphorylation. These *in vitro* results first suggested that the inhibition of haspin with LDN in control spermatocytes could cause centrosome instability and the appearance of multipolar M-I and M-II spermatocytes, pointing to a potential role of haspin in centrosome regulation in male mouse meiosis. In these multipolar metaphases, all induced MTOCs are capable of recruiting pericentrin and polymerizing microtubules, sharing similarities with somatic cells (Dai et al., 2009) and mouse oocytes (Balboula et al., 2016). However, we detected AURKAph at the poles of misaligned M-I and M-II in our *in vitro* studies with LDN treatment and in the mouse model *Haspin*$^{-/-}$, suggesting that haspin is not directly implicated in AURKA recruitment to centrosomes and it is not responsible for AURKA phosphorylation in spermatocytes, consistent with previous data in oocytes (Balboula et al., 2016). Moreover, as the small fraction of multipolar metaphases after haspin inhibition was detected in both control and *Haspin*$^{-/-}$ LDN-treated spermatocytes, we argue that unknown off-target effects of LDN could also have occurred in the *in vitro* experiments. It has been reported that several ATP-binding-site-targeting inhibitors have cross-reactivity between haspin and other protein kinases, the most common being the dual-specificity tyrosine-regulated kinases (DYRKs), a conserved family of protein kinases that phosphorylate a broad set of proteins involved in many different cellular processes, including centrosome regulation and ciliogenesis. In this regard, a high-throughput screen revealed that LDN exhibited potent inhibitory activity for proteins from the DYRK family (Cuny et al., 2010; Kestav et al., 2017). Given that DYRKs appear to contribute to the regulation of an array of signaling pathways, including cell cycle progression and mitosis (Yoshida and Yoshida, 2019), centrosome regulation and ciliogenesis (Hossain et al., 2017; Yoshida et al., 2020), we argue that the small proportion of multipolar spindles seen after LDN treatment could be an effect of DYRK, or other similar off-target protein kinase, alterations. Furthermore, as LDN has been approached as a therapeutic treatment in oncology (Amoussou et al., 2018), the importance of accurately designing therapies identifying the correct treatment concentrations and excluding off-target effects should be important in future studies to ensure the efficiency of these potential cures.

Haspin inhibition or ablation induces chromosomal mis-congression in male mouse meiosis but does not alter fertility

Haspin KO mitotic cell lines have been described to present delays in metaphase-anaphase progression due to bi-orientation errors and centromeric cohesion weakness (Zhou et al., 2014), whereas haspin inhibition induces chromosome mis-segregation, errors in congression and cytokinesis failure (Dai et al., 2009). In contrast, in mouse oocytes, A-I proceeds with chromosomes being mis-segregated and the persistence of improper kinetochore–microtubule attachments, yet cells complete cytokinesis and progress to M-II carrying aneuploidies (Kang et al., 2015; Nguyen et al., 2014; Quartuccio et al., 2017; Wang et al., 2016). We here found that LDN-inhibition of haspin in spermatocytes leads to a high incidence of misaligned metaphases, which could potentially cause aneuploid gametes. The *Haspin*$^{-/-}$ mouse model unravels the complexities of fully depleting the haspin kinase *in vitro* experimentally and confirmed haspin implication in chromosome congression. Nevertheless, *Haspin*$^{-/-}$ male mice present sperm in the epididymis, similarly to a previous *Haspin*$^{-/-}$ model (Shimada et al., 2016), indicating that although a high incidence of mis-segregation errors occurs during the first and the second meiotic division, spermatocytes progress to form mature gametes.

Altogether, the combined data regarding haspin inhibition in mitosis and meiosis are intriguing. The literature discussed shows that haspin inhibition leads to cell death in mitosis, but it does not interrupt meiosis; however, it needs to be considered that all these studies have been conducted *in vitro*, in which haspin is abruptly disrupted and might present a more aggressive phenotype. Our work combines the *in vitro* experiments with the characterization of the meiotic phenotype of a *Haspin*$^{-/-}$ mouse model, allowing us to conclude that the haspin kinase is dispensable for male mouse fertility.

MATERIALS AND METHODS

Mice

Testes from adult C57BL/6 (WT) and genetically modified *Haspin*$^{-/-}$ male mice were used for this study. All animal procedures were approved by local and regional ethics committees (Institutional Animal Care and Use Committee and Ethics Committee for Research and Animal Welfare, Instituto de Salud Carlos III) (permits PROEX 301/19) and performed according to the European Union guidelines for the protection of animals (2010/63/EU). The *Haspin* (*Gsg2*)-null allele, lacking the complete *Gsg2* single exon, was generated by the laboratory of M.M.

Culture of seminiferous tubules and LDN-192960 treatment

Culture of seminiferous tubules was performed as previously described (Alfaro et al., 2021; Sato et al., 2011). Testes from WT mice were removed, detunicated and fragments of seminiferous tubules were cultured in agarose gel half-soaked in Minimum Essential Medium α (MEMα; Gibco, A10490-01) supplemented with KnockOut Serum Replacement (KRS; Gibco, 10828-010) and antibiotics (penicillin/streptomycin; Biochrom AG, A2213) with 1 mM LDN-192960 (Sigma-Aldrich, SML0755), and were kept at 34°C in an atmosphere with 5% CO_2. Controls were kept in MEMα culture medium without LDN-192916. After 2, 4 and 6 h, control and inhibitor-treated seminiferous tubules were subjected to the squashing technique. The same treatment of 6 h 1 mM with LDN-192960 was performed with seminiferous tubules extracted from the *Haspin*$^{-/-}$ mouse model.

Immunofluorescence microscopy

Seminiferous tubules were fixed and processed following previously described protocols for squashing (Page et al., 1998; Parra et al., 2002) or spreading (Peters et al., 1997) techniques.

Kinetochores were revealed with a purified human anti-centromere autoantibody (ACA) serum (Antibodies Incorporated, 435-2RG-7) at a 1:20 dilution. SYCP3 was detected with either a mouse monoclonal antibody against mouse SYCP3 (Santa Cruz Biotechnology, sc-74569) or a rabbit polyclonal antibody recognizing mouse SYCP3 (Santa Cruz Biotechnology, sc-33195), both at a 1:50 dilution. Histone modifications were detected with the following primary antibodies: rabbit polyclonal anti-H2AT120ph antibody (Active Motif, 39391) at a 1:10 dilution, rabbit polyclonal anti-H3T3ph antibodies (Abcam, ab-17532; and Upstate, 07-424) at a 1:800 dilution, and rabbit polyclonal anti-H3S10ph antibody (Merck Millipore, 06-570) at a 1:100 dilution. AURKB was detected with a mouse monoclonal anti-Aurora B (AIM-1) antibody (BD Biosciences, 611082) at a 1:30 dilution, and AURKB/Cph were revealed with a rabbit polyclonal anti-AuroraTph antibody (Cell Signaling, 2914S) at a 1:30 dilution. Shugoshin 2 (SGO2) was revealed with a rabbit polyclonal anti-SGO2 antibody generated by Dr José Luis Barbero (CIB-CSIC, Spain) (Gómez et al., 2007). Rabbit polyclonal anti-borealin antibody was generously provided by Dr William Earnshaw (University of Edinburgh, UK) (Gassmann et al., 2004) and was used at a 1:50 dilution. Sheep polyclonal anti-MCAK antibody was generously provided by Dr Linda Wordeman (University of Wasington, USA) (Maney et al., 1998) and used at a 1:40 dilution. Tubulin was detected with a rat anti-α-tubulin antibody (Abcam, ab6160) at a 1:100 dilution. Pericentrin (PCNT) was

detected with a rabbit polyclonal antibody (Abcam, ab4448) at a 1:30 dilution. Centrin 3 (CETN3) was detected with a mouse monoclonal antibody (Novus Biologicals, H00001070-M01) at 1:100 dilution. SMC3 was detected with a rabbit polyclonal antibody (Abcam, ab9263) at a 1:30 dilution. Corresponding secondary antibodies were used against rabbit, mouse, rat, sheep and human IgGs conjugated with either Texas Red (Jackson ImmunoResearch), Alexa Fluor 594 or Alexa Fluor 488 (Molecular Probes), all of them used at a 1:100 dilution.

After several tries with three different commercial antibodies (Santa Cruz Biotechnology, sc-98.622; Abnova, H00083903-B01P; and Bethyl Laboratories, A302-241A) and two custom-made antibodies, we could not obtain an antibody that accurately shows the distribution of haspin in mouse spermatocytes.

Immunofluorescence images and stacks were collected on an Olympus BX61 microscope equipped with epifluorescence optics, a motorized *z*-drive, and Olympus DP71 or DP70 digital cameras controlled by analySIS software (Soft Imaging System). Finally, images were processed with ImageJ (National Institutes of Health, USA; http://rsb.info.nih.gov/ij) and/or Adobe Photoshop softwares.

Apoptosis marker

The DNA fragmentation-associated apoptosis in spermatocytes was detected by the TUNEL assay by using a commercial kit (Roche, 11684795910) according to the manufacturer's protocol. Nuclei were counterstained for 3 min with 10 µg/ml DAPI. Tests were developed on formaldehyde-fixed seminiferous tubules.

Sperm chromatin dispersion assay

Quantification of DNA fragmentation of mice sperm was performed following the instructions of the Halosperm kit (Halotech DNA SL, HT-HS10) and revealed with the Fluogreen kit (Halotech, HT-GFS100).

Histology

For histological sections, testes were fixed in 10% buffered formalin (Sigma-Aldrich) and embedded in paraffin wax. After standard washes and dehydration, paraplast-embedded tissue blocks were cut in 3–5 µm-thick sections in a Reichert microtome. Finally, sections were stained with Hematoxylin and Eosin.

Quantification and statistical analysis

Quantification of the immunofluorescence intensity was estimated by measuring the integrated fluorescence density in individual nuclei using ImageJ by creating a binary mask with the DAPI staining. The acquisition time was fixed for all acquired images, and the quantification was only performed using the original unmodified images. A minimum of ten metaphase spermatocytes per condition were analyzed in each experiment. All graphics and statistical tests were performed with GraphPad Prism 9.0 software. Mean differences for each group were evaluated by an independent sample two-tailed unpaired *t*-test. Values are expressed as mean±s.e.m. and *P*-values below 0.05 were considered statistically significant.

Acknowledgements

We express our sincere thanks to José Luis Barbero, William Earnshaw and Linda Wordeman for providing antibodies; to Katja Wassmann, Carlos Dotti and Carmen López Fernández for scientific support; and to Lorena Barreras for technical assistance.

Competing interests

The authors declare no competing or financial interests.

Author contributions

Conceptualization: I.B., P.L.-J., A.V., J.P., C.M., M.M., J.A.S., R.G.; Methodology: I.B., P.L.-J., I.M., J.G.-M., C.M., R.G.; Software: I.B., P.L.-J.; Validation: I.B., P.L.-J., J.G.-M., M.M., J.A.S., R.G.; Formal analysis: I.B., P.L.-J., I.M., C.M., M.M., J.A.S., R.G.; Investigation: I.B., P.L.-J., I.M., J.G.-M., C.M., M.M., J.A.S., R.G.; Resources: M.M., J.P., J.A.S., R.G.; Data curation: I.B., P.L.-J., C.M., R.G.; Writing - original draft: I.B., R.G., P.L-J.; Writing - review & editing: I.B., P.L.-J., A.V., J.P., C.M., M.M., J.A.S., R.G.; Visualization: I.B., P.L.-J., R.G.; Supervision: M.M., J.A.S., R.G.; Project administration: M.M., J.A.S., R.G.; Funding acquisition: J.P., R.G., M.M., J.A.S.

Funding

This work was funded by Ministerio de Economía y Competitividad and Ministerio de Ciencia e Innovación (Spain) (PID2020-117491GB-I00 to J.A.S.; RTI2018-095582-B-I00 to M.M.; CGL2014-53106-P to J.P., and BIOUAM02-2020 to J.P. and R.G.). I.B and J.G.-M. were supported by grant FPI of Ministerio de Economía, Industria y Competitividad (Spain). C.M. was supported by Juan de la Cierva programme of Ministerio de Economía, Industria y Competitividad and by Centro Nacional de Investigaciones Oncológicas (CNIO) Friends Postdoctoral Programme (Spain).

References

Alfaro, E., López-Jiménez, P., González-Martínez, J., Malumbres, M., Suja, J. A. and Gómez, R. (2021). PLK1 regulates centrosome migration and spindle dynamics in male mouse meiosis. *EMBO Rep.* **22**, e51030. doi:10.15252/embr.202051030

Amoussou, N. G., Bigot, A., Roussakis, C. and Robert, J.-M. H. (2018). Haspin: a promising target for the design of inhibitors as potent anticancer drugs. *Drug Discov. Today* **23**, 409-415. doi:10.1016/j.drudis.2017.10.005

Andrews, P. D., Ovechkina, Y., Morrice, N., Wagenbach, M., Duncan, K., Wordeman, L. and Swedlow, J. R. (2004). Aurora B regulates MCAK at the mitotic centromere. *Dev. Cell* **6**, 253-268. doi:10.1016/S1534-5807(04)00025-5

Balboula, A. Z. and Schindler, K. (2014). Selective disruption of aurora C kinase reveals distinct functions from aurora B kinase during meiosis in mouse oocytes. *PLoS Genet.* **10**, e1004194. doi:10.1371/journal.pgen.1004194

Balboula, A. Z., Nguyen, A. L., Gentilello, A. S., Quartuccio, S. M., Drutovic, D., Solc, P. and Schindler, K. (2016). Haspin kinase regulates microtubule-organizing center clustering and stability through Aurora kinase C in mouse oocytes. *J. Cell Sci.* **129**, 3648-3660. doi:10.1242/jcs.189340

Broad, A. J., DeLuca, K. F. and DeLuca, J. G. (2020). Aurora B kinase is recruited to multiple discrete kinetochore and centromere regions in human cells. *J. Cell Biol.* **219**, e201905144. doi:10.1083/jcb.201905144

Brown, J. R., Koretke, K. K., Birkeland, M. L., Sanseau, P. and Patrick, D. R. (2004). Evolutionary relationships of Aurora kinases: implications for model organism studies and the development of anti-cancer drugs. *BMC Evol. Biol.* **4**, 39. doi:10.1186/1471-2148-4-39

Cairo, G. and Lacefield, S. (2020). Establishing correct kinetochore-microtubule attachments in mitosis and meiosis. *Essays Biochem.* **64**, 277-287. doi:10.1042/EBC20190072

Cao, Z., Xu, T., Tong, X., Zhang, D., Liu, C., Wang, Y., Gao, D., Luo, L., Zhang, L., Li, Y. et al. (2019). HASPIN kinase mediates histone deacetylation to regulate oocyte meiotic maturation in pigs. *Reproduction* **157**, 501-510. doi:10.1530/REP-18-0447

Carretero, M., Ruiz-Torres, M., Rodríguez-Corsino, M., Barthelemy, I. and Losada, A. (2013). Pds5B is required for cohesion establishment and Aurora B accumulation at centromeres. *EMBO J.* **32**, 2938-2949. doi:10.1038/emboj.2013.230

Chen, A., Wen, S., Liu, F., Zhang, Z., Liu, M., Wu, Y., He, B., Yan, M., Kang, T., Lam, E. W. F. et al. (2021). CRISPR/Cas9 screening identifies a kinetochore-microtubule dependent mechanism for Aurora-A inhibitor resistance in breast cancer. *Cancer Commun. (Lond)* **41**, 121-139. doi:10.1002/cac2.12125

Cuny, G. D., Robin, M., Ulyanova, N. P., Patnaik, D., Pique, V., Casano, G., Liu, J.-F., Lin, X., Xian, J., Glicksman, M. A. et al. (2010). Structure-activity relationship study of acridine analogs as haspin and DYRK2 kinase inhibitors. *Bioorg. Med. Chem. Lett.* **20**, 3491-3494. doi:10.1016/j.bmcl.2010.04.150

Cuny, G. D., Ulyanova, N. P., Patnaik, D., Liu, J.-F., Lin, X., Auerbach, K., Ray, S. S., Xian, J., Glicksman, M. A., Stein, R. L. et al. (2012). Structure-activity relationship study of beta-carboline derivatives as haspin kinase inhibitors. *Bioorg. Med. Chem. Lett.* **22**, 2015-2019. doi:10.1016/j.bmcl.2012.01.028

Dai, J. and Higgins, J. M. G. (2005). Haspin: a mitotic histone kinase required for metaphase chromosome alignment. *Cell Cycle* **4**, 665-668. doi:10.4161/cc.4.5.1683

Dai, J., Sultan, S., Taylor, S. S. and Higgins, J. M. G. (2005). The kinase haspin is required for mitotic histone H3 Thr 3 phosphorylation and normal metaphase chromosome alignment. *Genes Dev.* **19**, 472-488. doi:10.1101/gad.1267105

Dai, J., Sullivan, B. A. and Higgins, J. M. G. (2006). Regulation of mitotic chromosome cohesion by Haspin and Aurora B. *Dev. Cell* **11**, 741-750. doi:10.1016/j.devcel.2006.09.018

Dai, J., Kateneva, A. V. and Higgins, J. M. G. (2009). Studies of haspin-depleted cells reveal that spindle-pole integrity in mitosis requires chromosome cohesion. *J. Cell Sci.* **122**, 4168-4176. doi:10.1242/jcs.054122

De Antoni, A., Maffini, S., Knapp, S., Musacchio, A. and Santaguida, S. (2012). A small-molecule inhibitor of Haspin alters the kinetochore functions of Aurora B. *J. Cell Biol.* **199**, 269-284. doi:10.1083/jcb.201205119

El Yakoubi, W., Buffin, E., Cladière, D., Gryaznova, Y., Berenguer, I., Touati, S. A., Gómez, R., Suja, J. A., van Deursen, J. M. and Wassmann, K. (2017). Mps1 kinase-dependent Sgo2 centromere localisation mediates cohesin protection in mouse oocyte meiosis I. *Nat. Commun.* **8**, 694. doi:10.1038/s41467-017-00774-3

Gassmann, R., Carvalho, A., Henzing, A. J., Ruchaud, S., Hudson, D. F., Honda, R., Nigg, E. A., Gerloff, D. L. and Earnshaw, W. C. (2004). Borealin: a

novel chromosomal passenger required for stability of the bipolar mitotic spindle. *J. Cell Biol.* **166**, 179-191. doi:10.1083/jcb.200404001

Ghenoiu, C., Wheelock, M. S. and Funabiki, H. (2013). Autoinhibition and Polo-dependent multisite phosphorylation restrict activity of the histone H3 kinase Haspin to mitosis. *Mol. Cell* **52**, 734-745. doi:10.1016/j.molcel.2013.10.002

Gómez, R., Valdeolmillos, A., Parra, M. T., Viera, A., Carreiro, C., Roncal, F., Rufas, J. S., Barbero, J. L. and Suja, J. A. (2007). Mammalian SGO2 appears at the inner centromere domain and redistributes depending on tension across centromeres during meiosis II and mitosis. *EMBO Rep.* **8**, 173-180. doi:10.1038/sj.embor.7400877

Gorbsky, G. J. (2004). Mitosis: MCAK under the aura of Aurora B. *Curr. Biol.* **14**, R346-R348. doi:10.1016/j.cub.2004.04.022

Hadders, M. A., Hindriksen, S., Truong, M. A., Mhaskar, A. N., Wopken, J. P., Vromans, M. J. M. and Lens, S. M. A. (2020). Untangling the contribution of Haspin and Bub1 to Aurora B function during mitosis. *J. Cell Biol.* **219**, e201907087. doi:10.1083/jcb.201907087

Higgins, J. M. G. (2010). Haspin: a newly discovered regulator of mitotic chromosome behavior. *Chromosoma* **119**, 137-147. doi:10.1007/s00412-009-0250-4

Hindriksen, S., Lens, S. M. A. and Hadders, M. A. (2017). The ins and outs of aurora B inner centromere localization. *Front. Cell Dev. Biol.* **5**, 112. doi:10.3389/fcell.2017.00112

Hirota, T., Lipp, J. J., Toh, B.-H. and Peters, J.-M. (2005). Histone H3 serine 10 phosphorylation by Aurora B causes HP1 dissociation from heterochromatin. *Nature* **438**, 1176-1180. doi:10.1038/nature04254

Hossain, D., Javadi Esfehani, Y., Das, A. and Tsang, W. Y. (2017). Cep78 controls centrosome homeostasis by inhibiting EDD-DYRK2-DDB1(Vpr)(BP). *EMBO Rep.* **18**, 632-644. doi:10.15252/embr.201642377

Huang, H., Feng, J., Famulski, J., Rattner, J. B., Liu, S. T., Kao, G. D., Muschel, R., Chan, G. K. T. and Yen, T. J. (2007). Tripin/hSgo2 recruits MCAK to the inner centromere to correct defective kinetochore attachments. *J. Cell Biol.* **177**, 413-424. doi:10.1083/jcb.200701122

Huertas, D., Soler, M., Moreto, J., Villanueva, A., Martinez, A., Vidal, A., Charlton, M., Moffat, D., Patel, S., McDermott, J. et al. (2012). Antitumor activity of a small-molecule inhibitor of the histone kinase Haspin. *Oncogene* **31**, 1408-1418. doi:10.1038/onc.2011.335

Kang, H., Park, Y. S., Cho, D.-H., Kim, J.-S. and Oh, J. S. (2015). Dynamics of histone H3 phosphorylation at threonine 3 during meiotic maturation in mouse oocytes. *Biochem. Biophys. Res. Commun.* **458**, 280-286. doi:10.1016/j.bbrc.2015.01.099

Kawashima, S. A., Yamagishi, Y., Honda, T., Ishiguro, K. and Watanabe, Y. (2010). Phosphorylation of H2A by Bub1 prevents chromosomal instability through localizing shugoshin. *Science* **327**, 172-177. doi:10.1126/science.1180189

Kelly, A. E., Ghenoiu, C., Xue, J. Z., Zierhut, C., Kimura, H. and Funabiki, H. (2010). Survivin reads phosphorylated histone H3 threonine 3 to activate the mitotic kinase Aurora B. *Science* **330**, 235-239. doi:10.1126/science.1189505

Kestav, K., Uri, A. and Lavogina, D. (2017). Structure, roles and inhibitors of a mitotic protein kinase haspin. *Curr. Med. Chem.* **24**, 2276-2293. doi:10.2174/0929867324666170414155520

Kline-Smith, S. L. and Walczak, C. E. (2004). Mitotic spindle assembly and chromosome segregation: refocusing on microtubule dynamics. *Mol. Cell* **15**, 317-327. doi:10.1016/j.molcel.2004.07.012

Kozgunova, E., Suzuki, T., Ito, M., Higashiyama, T. and Kurihara, D. (2016). Haspin has multiple functions in the plant cell division regulatory network. *Plant Cell Physiol.* **57**, 848-861. doi:10.1093/pcp/pcw030

Krenn, V. and Musacchio, A. (2015). The aurora B kinase in chromosome bi-orientation and spindle checkpoint signaling. *Front. Oncol.* **5**, 225. doi:10.3389/fonc.2015.00225

Lan, W., Zhang, X., Kline-Smith, S. L., Rosasco, S. E., Barrett-Wilt, G. A., Shabanowitz, J., Hunt, D. F., Walczak, C. E. and Stukenberg, P. T. (2004). Aurora B phosphorylates centromeric MCAK and regulates its localization and microtubule depolymerization activity. *Curr. Biol.* **14**, 273-286. doi:10.1016/j.cub.2004.01.055

Liang, C., Chen, Q., Yi, Q., Zhang, M., Yan, H., Zhang, B., Zhou, L., Zhang, Z., Qi, F., Ye, S. et al. (2018). A kinase-dependent role for Haspin in antagonizing Wapl and protecting mitotic centromere cohesion. *EMBO Rep.* **19**, 43-56. doi:10.15252/embr.201744737

Liang, C., Zhang, Z., Chen, Q., Yan, H., Zhang, M., Zhou, L., Xu, J., Lu, W. and Wang, F. (2020). Centromere-localized Aurora B kinase is required for the fidelity of chromosome segregation. *J. Cell Biol.* **219**, e201907092. doi:10.1083/jcb.201907092

Llano, E., Gómez, R., Gutiérrez-Caballero, C., Herrán, Y., Sánchez-Martín, M., Vázquez-Quiñones, L., Hernández, T., de Álava, E., Cuadrado, A., Barbero, J. L. et al. (2008). Shugoshin-2 is essential for the completion of meiosis but not for mitotic cell division in mice. *Genes Dev.* **22**, 2400-2413. doi:10.1101/gad.475308

Lukasiewicz, K. B. and Lingle, W. L. (2009). Aurora A, centrosome structure, and the centrosome cycle. *Environ. Mol. Mutagen.* **50**, 602-619. doi:10.1002/em.20533

Maiolica, A., de Medina-Redondo, M., Schoof, E. M., Chaikuad, A., Villa, F., Gatti, M., Jeganathan, S., Lou, H. J., Novy, K., Hauri, S. et al. (2014). Modulation of the chromatin phosphoproteome by the Haspin protein kinase. *Mol. Cell. Proteomics* **13**, 1724-1740. doi:10.1074/mcp.M113.034819

Maney, T., Hunter, A. W., Wagenbach, M. and Wordeman, L. (1998). Mitotic centromere-associated kinesin is important for anaphase chromosome segregation. *J. Cell Biol.* **142**, 787-801. doi:10.1083/jcb.142.3.787

Markaki, Y., Christogianni, A., Politou, A. S. and Georgatos, S. D. (2009). Phosphorylation of histone H3 at Thr3 is part of a combinatorial pattern that marks and configures mitotic chromatin. *J. Cell Sci.* **122**, 2809-2819. doi:10.1242/jcs.043810

McHugh, T., Zou, J., Volkov, V. A., Bertin, A., Talapatra, S. K., Rappsilber, J., Dogterom, M. and Welburn, J. P. I. (2019). The depolymerase activity of MCAK shows a graded response to Aurora B kinase phosphorylation through allosteric regulation. *J. Cell Sci.* **132**, jcs228353. doi:10.1242/jcs.228353

Nguyen, A. L. and Schindler, K. (2017). Specialize and divide (Twice): functions of three aurora kinase homologs in mammalian oocyte meiotic maturation. *Trends Genet.* **33**, 349-363. doi:10.1016/j.tig.2017.03.005

Nguyen, A. L., Gentilello, A. S., Balboula, A. Z., Shrivastava, V., Ohring, J. and Schindler, K. (2014). Phosphorylation of threonine 3 on histone H3 by haspin kinase is required for meiosis I in mouse oocytes. *J. Cell Sci.* **127**, 5066-5078. doi:10.1242/jcs.158840

Nguyen, A. L., Drutovic, D., Vazquez, B. N., El Yakoubi, W., Gentilello, A. S., Malumbres, M., Solc, P. and Schindler, K. (2018). Genetic Interactions between the Aurora Kinases Reveal New Requirements for AURKB and AURKC during Oocyte Meiosis. *Curr. Biol.* **28**, 3458-3468.e55. doi:10.1016/j.cub.2018.08.052

Nikonova, A. S., Astsaturov, I., Serebriiskii, I. G., Dunbrack, R. L., Jr and Golemis, E. A. (2013). Aurora A kinase (AURKA) in normal and pathological cell division. *Cell. Mol. Life Sci.* **70**, 661-687 doi:10.1007/s00018-012-1073-7

Ohi, R., Sapra, T., Howard, J. and Mitchison, T. J. (2004). Differentiation of cytoplasmic and meiotic spindle assembly MCAK functions by Aurora B-dependent phosphorylation. *Mol. Biol. Cell* **15**, 2895-2906. doi:10.1091/mbc.e04-02-0082

Page, J., Suja, J. A., Santos, J. L. and Rufas, J. S. (1998). Squash procedure for protein immunolocalization in meiotic cells. *Chromosome Res.* **6**, 639-642. doi:10.1023/A:1009209628300

Parra, M. T., Page, J., Yen, T. J., He, D., Valdeolmillos, A., Rufas, J. S. and Suja, J. A. (2002). Expression and behaviour of CENP-E at kinetochores during mouse spermatogenesis. *Chromosoma* **111**, 53-61. doi:10.1007/s00412-002-0185-5

Parra, M. T., Viera, A., Gómez, R., Page, J., Carmena, M., Earnshaw, W. C., Rufas, J. S. and Suja, J. A. (2003). Dynamic relocalization of the chromosomal passenger complex proteins inner centromere protein (INCENP) and aurora-B kinase during male mouse meiosis. *J. Cell Sci.* **116**, 961-974. doi:10.1242/jcs.00330

Parra, M. T., Viera, A., Gómez, R., Page, J., Benavente, R., Santos, J. L., Rufas, J. S. and Suja, J. A. (2004). Involvement of the cohesin Rad21 and SCP3 in monopolar attachment of sister kinetochores during mouse meiosis I. *J. Cell Sci.* **117**, 1221-1234. doi:10.1242/jcs.00947

Parra, M. T., Gómez, R., Viera, A., Page, J., Calvente, A., Wordeman, L., Rufas, J. S. and Suja, J. A. (2006). A perikinetochoric ring defined by MCAK and Aurora-B as a novel centromere domain. *PLoS Genet.* **2**, e84. doi:10.1371/journal.pgen.0020084

Parra, M. T., Gómez, R., Viera, A., Llano, E., Pendás, A. M., Rufas, J. S. and Suja, J. A. (2009). Sequential assembly of centromeric proteins in male mouse meiosis. *PLoS Genet.* **5**, e1000417. doi:10.1371/journal.pgen.1000417

Patnaik, D., Jun, X., Glicksman, M. A., Cuny, G. D., Stein, R. L. and Higgins, J. M. (2008). Identification of small molecule inhibitors of the mitotic kinase haspin by high-throughput screening using a homogeneous time-resolved fluorescence resonance energy transfer assay. *J. Biomol. Screen.* **13**, 1025-1034. doi:10.1177/1087057108326081

Peters, A. H. F. M., Plug, A. W., van Vugt, M. J. and de Boer, P. (1997). A drying-down technique for the spreading of mammalian meiocytes from the male and female germline. *Chromosome Res.* **5**, 66-68. doi:10.1023/A:1018445520117

Qian, J., Beullens, M., Lesage, B. and Bollen, M. (2013). Aurora B defines its own chromosomal targeting by opposing the recruitment of the phosphatase scaffold Repo-Man. *Curr. Biol.* **23**, 1136-1143. doi:10.1016/j.cub.2013.05.017

Qiao, J., Wang, Z.-B., Feng, H.-L., Miao, Y.-L., Wang, Q., Yu, Y., Wei, Y.-C., Yan, J., Wang, W.-H., Shen, W. et al. (2014). The root of reduced fertility in aged women and possible therapentic options: current status and future perspects. *Mol. Aspects Med.* **38**, 54-85. doi:10.1016/j.mam.2013.06.001

Quartuccio, S. M., Dipali, S. S. and Schindler, K. (2017). Haspin inhibition reveals functional differences of interchromatid axis-localized AURKB and AURKC. *Mol. Biol. Cell* **28**, 2233-2240. doi:10.1091/mbc.e16-12-0850

Ritter, A., Kreis, N.-N., Louwen, F., Wordeman, L. and Yuan, J. (2015). Molecular insight into the regulation and function of MCAK. *Crit. Rev. Biochem. Mol. Biol.* **51**, 228-245. doi:10.1080/10409238.2016.1178705

Ruchaud, S., Carmena, M. and Earnshaw, W. C. (2007). Chromosomal passengers: conducting cell division. *Nat. Rev. Mol. Cell Biol.* **8**, 798-812. doi:10.1038/nrm2257

Ruppert, J. G., Samejima, K., Platani, M., Molina, O., Kimura, H., Jeyaprakash, A. A., Ohta, S. and Earnshaw, W. C. (2018). HP1α targets the chromosomal passenger complex for activation at heterochromatin before mitotic entry. *EMBO J.* **37**, e97677. doi:10.15252/embj.201797677

Santaguida, S., Tighe, A., D'Alise, A. M., Taylor, S. S. and Musacchio, A. (2010). Dissecting the role of MPS1 in chromosome biorientation and the spindle checkpoint through the small molecule inhibitor reversine. *J. Cell Biol.* **190**, 73-87. doi:10.1083/jcb.201001036

Sato, T., Katagiri, K., Yokonishi, T., Kubota, Y., Inoue, K., Ogonuki, N., Matoba, S., Ogura, A. and Ogawa, T. (2011). In vitro production of fertile sperm from murine spermatogonial stem cell lines. *Nat. Commun.* **2**, 472. doi:10.1038/ncomms1478

Saurin, A. T., van der Waal, M. S., Medema, R. H., Lens, S. M. A. and Kops, G. J. (2011). Aurora B potentiates Mps1 activation to ensure rapid checkpoint establishment at the onset of mitosis. *Nat. Commun.* **2**, 316. doi:10.1038/ncomms1319

Schmucker, S. and Sumara, I. (2014). Molecular dynamics of PLK1 during mitosis. *Mol. Cell Oncol.* **1**, e954507. doi:10.1080/23723548.2014.954507

Shimada, M., Goshima, T., Matsuo, H., Johmura, Y., Haruta, M., Murata, K., Tanaka, H., Ikawa, M., Nakanishi, K. and Nakanishi, M. (2016). Essential role of autoactivation circuitry on Aurora B-mediated H2AX-pS121 in mitosis. *Nat. Commun.* **7**, 12059. doi:10.1038/ncomms12059

Shuda, K., Schindler, K., Ma, J., Schultz, R. M. and Donovan, P. J. (2009). Aurora kinase B modulates chromosome alignment in mouse oocytes. *Mol. Reprod. Dev.* **76**, 1094-1105. doi:10.1002/mrd.21075

Soupsana, K., Karanika, E., Kiosse, F., Christogianni, A., Sfikas, Y., Topalis, P., Batistatou, A., Kanaki, Z., Klinakis, A., Politou, A. S. et al. (2021). Distinct roles of haspin in stem cell division and male gametogenesis. *Sci. Rep.* **11**, 19901. doi:10.1038/s41598-021-99307-8

Tanaka, H., Yoshimura, Y., Nozaki, M., Yomogida, K., Tsuchida, J., Tosaka, Y., Habu, T., Nakanishi, T., Okada, M., Nojima, H. et al. (1999). Identification and characterization of a haploid germ cell-specific nuclear protein kinase (Haspin) in spermatid nuclei and its effects on somatic cells. *J. Biol. Chem.* **274**, 17049-17057. doi:10.1074/jbc.274.24.17049

Tang, A., Gao, K., Chu, L., Zhang, R., Yang, J. and Zheng, J. (2017). Aurora kinases: novel therapy targets in cancers. *Oncotarget* **8**, 23937-23954. doi:10.18632/oncotarget.14893

Tanno, Y., Kitajima, T. S., Honda, T., Ando, Y., Ishiguro, K.-I. and Watanabe, Y. (2010). Phosphorylation of mammalian Sgo2 by Aurora B recruits PP2A and MCAK to centromeres. *Genes Dev.* **24**, 2169-2179. doi:10.1101/gad.1945310

Trivedi, P. and Stukenberg, P. T. (2020). A condensed view of the chromosome passenger complex. *Trends Cell Biol.* **30**, 676-687. doi:10.1016/j.tcb.2020.06.005

Vagnarelli, P., Ribeiro, S., Sennels, L., Sanchez-Pulido, L., de Lima Alves, F., Verheyen, T., Kelly, D. A., Ponting, C. P., Rappsilber, J. and Earnshaw, W. C. (2011). Repo-Man coordinates chromosomal reorganization with nuclear envelope reassembly during mitotic exit. *Dev. Cell* **21**, 328-342. doi:10.1016/j.devcel.2011.06.020

van der Horst, A., Vromans, M. J. M., Bouwman, K., van der Waal, M. S., Hadders, M. A. and Lens, S. M. A. (2015). Inter-domain cooperation in INCENP promotes aurora B relocation from centromeres to microtubules. *Cell Rep.* **12**, 380-387. doi:10.1016/j.celrep.2015.06.038

Wang, F., Dai, J., Daum, J. R., Niedzialkowska, E., Banerjee, B., Stukenberg, P. T., Gorbsky, G. J. and Higgins, J. M. G. (2010). Histone H3 Thr-3 phosphorylation by Haspin positions Aurora B at centromeres in mitosis. *Science* **330**, 231-235. doi:10.1126/science.1189435

Wang, F., Ulyanova, N. P., van der Waal, M. S., Patnaik, D., Lens, S. M. A. and Higgins, J. M. G. (2011). A positive feedback loop involving Haspin and Aurora B promotes CPC accumulation at centromeres in mitosis. *Curr. Biol.* **21**, 1061-1069. doi:10.1016/j.cub.2011.05.016

Wang, F., Ulyanova, N. P., Daum, J. R., Patnaik, D., Kateneva, A. V., Gorbsky, G. J. and Higgins, J. M. G. (2012). Haspin inhibitors reveal centromeric functions of Aurora B in chromosome segregation. *J. Cell Biol.* **199**, 251-268. doi:10.1083/jcb.201205106

Wang, Q., Wei, H., Du, J., Cao, Y., Zhang, N., Liu, X., Liu, X., Chen, D. and Ma, W. (2016). H3 Thr3 phosphorylation is crucial for meiotic resumption and anaphase onset in oocyte meiosis. *Cell Cycle* **15**, 213-224. doi:10.1080/15384101.2015.1121330

Wellard, S. R., Schindler, K. and Jordan, P. W. (2020). Aurora B and C kinases regulate chromosome desynapsis and segregation during mouse and human spermatogenesis. *J. Cell Sci.* **133**, jcs248831. doi:10.1242/jcs.248831

Wellard, S. R., Zhang, Y., Shults, C., Zhao, X., McKay, M., Murray, S. A. and Jordan, P. W. (2021). Overlapping roles for PLK1 and Aurora A during meiotic centrosome biogenesis in mouse spermatocytes. *EMBO Rep.* **22**, e51023. doi:10.15252/embr.202154106

Yamagishi, Y., Honda, T., Tanno, Y. and Watanabe, Y. (2010). Two histone marks establish the inner centromere and chromosome bi-orientation. *Science* **330**, 239-243. doi:10.1126/science.1194498

Yoshida, S. and Yoshida, K. (2019). Multiple functions of DYRK2 in cancer and tissue development. *FEBS Lett.* **593**, 2953-2965. doi:10.1002/1873-3468.13601

Yoshida, S., Aoki, K., Fujiwara, K., Nakakura, T., Kawamura, A., Yamada, K., Ono, M., Yogosawa, S. and Yoshida, K. (2020). The novel ciliogenesis regulator DYRK2 governs Hedgehog signaling during mouse embryogenesis. *eLife* **9**, e57381. doi:10.7554/eLife.57381

Zhou, L., Tian, X., Zhu, C., Wang, F. and Higgins, J. M. G. (2014). Polo-like kinase-1 triggers histone phosphorylation by Haspin in mitosis. *EMBO Rep.* **15**, 273-281. doi:10.1002/embr.201338080

Zhu, D., Gu, X., Lin, Z., Yu, D., Wang, J. and Li, L. (2020). HASPIN is involved in the progression of gallbladder carcinoma. *Exp. Cell Res.* **390**, 111863. doi:10.1016/j.yexcr.2020.111863